Duane's Ophthalmology, 2009 Edition
Tasman and Jaeger, Editors
Lippincott Williams & Wilkins

Functional Neuroanatomy of the Retina

Robert E. Marc

Department of Ophthalmology, Moran Eye Center, University of Utah;
65 Mario Capecchi Dr., Salt Lake City 84132 UT
robert.marc@hsc.utah.edu

Prologue

In the eight years since Dr. Paul Witkovsky reviewed retinal anatomy and function for this series, a sea change has occurred. We have progressively uncovered detailed molecular architectures for many structures and processes. We have concretely linked circuitry and retinal disease. There is now an overwhelming amount of literature to be screened. A PubMed search on the topic of "retina AND neuron" over 2001-2008 retrieves > 10,000 papers. If you started today and read all day, every day without fail, it would take two-to-three years to catch up to 2008, and then you would still be three years behind an exponentially growing field. After severe winnowing the reference list has grown to over 250 papers, yet it is certain that I have neglected key publications. I apologize to those authors in advance. What justifies this expansion? First, we have now assembled a nearly complete catalogue of cells in the retina (perhaps 90%) and have learned a tremendous amount about neuronal phenotypes and connections. We simultaneously know more and, paradoxically, understand less about primate color coding mechanisms. New retinal cell types have been discovered and refined models of synaptic signaling have emerged. Our understanding of the molecular mechanisms of synaptic function, of neurotransmitter receptor molecular biology, of modulatory mechanisms, and gap junctions has exploded. Further, we now have strong evidence of postnatal and disease-induced neuroplasticity in the mature retina. Some problems persist. We still do not know how horizontal cells (HCs) work; how red/green color coding happens; why we need so many kinds of bipolar cells (BCs) and amacrine cells (ACs); how the retina develops (though great advances have been made); what retinal efferents do; nor the exact details of any ganglion cell (GC) micronetwork. The study of retinal structure remains a dynamic, challenging enterprise.

Introduction

The vertebrate retina encodes visual scenes in starlight and at the solar zenith, discriminates spectral reflectances, detects motion, outlines form, and even mediates non-imaging-forming light encoding in some species. Most vertebrate retinas are duplex, using rod photoreceptors for nocturnal scotopic vision and cones for diurnal photopic vision. Our focus will be the mammalian retina in general, and the primate retina in particular. While the mammalian retina is complex, it is a *reduced and re-derived* vertebrate retina with less neuronal diversity and sensory bandwidth than those of avians, reptiles, amphibians and fishes. The evolutionary mechanisms underlying this reduction are

beyond the scope of this chapter, but every mammalian attribute ought to be viewed in the light of this evolutionary transformation.

Functional neuroanatomy addresses not only the neuronal architecture of signal processing, but also the synaptic connectivity, network topology, and signaling biophysics of retinal networks. The retina has been the focus of intense investigation since the earliest days of neuroanatomical research. The great Spanish neuroanatomist Santiago Ramón y Cajal, who shared 1906 Nobel Prize for Medicine with Camillo Golgi (and whose methods he used) set forth reasons for the attractiveness of the retina as an experimental tissue in the introduction to his classic study (1): the basic flow of information from photoreceptors toward ganglion cells was largely understood; the retinal neurons were arrayed in well-defined cellular layers; their contacts with other neurons were separated into clear zones (the inner and outer plexiform layers); and the compact nature of a cell's dendritic and axonal arbors facilitated study of its nervous connections. Ramón y Cajal considered the retina to be a true nervous center, but one whose thinness and transparency made it ideal for histologic analysis.

We still find this framework essential, but there is much molecular and structural information to add. In addition to new imaging and electrophysiological tools, we add increasingly detailed descriptions of molecular networks that participate in retinal signaling, growth, normal and pathologic function, and cell death. One important and clinically potent finding is that the nervous system, including the retina, is highly plastic. In addition to the basic "hard-wiring" of the system, parallel arrays of neuromodulators (2, 3) such as peptides, amines, metabolites and even free gases modify the properties of circuits. Neuromodulation is predominantly linked through transmembrane signaling systems, usually G-protein coupled receptors (GPCRs) whose transduction networks converge on a variety of intracellular proteins (e.g., kinases), which exert subtle control over target receptors and channels. In most cases neuromodulators reach their targets by diffusion from distant sources (4). Of high clinical import for translational work is the discovery that the retina is plastic under pathologic conditions, displaying structural remodeling, physical rewiring and molecular reprogramming, requiring a new neuroscience-based understanding of these diseases. Neural circuitry is no longer simply the playground of the *cognoscenti* but a fundamental part of medical praxis.

Ramón y Cajal (1) and Stephen Polyak (5) catalogued the fundamental shapes and laminar locations of a given cell's dendritic and axonal arborizations. To this we now add the display of electrical and chemical synapses among neurons, neurotransmitter and receptor expression patterns, new mechanisms of signal integration, plasticity / adaptation and developmental history. This chapter reviews many of these topics and (i) considers persistent problems, (ii) addresses revisions in our thinking about specific networks, and (iii) summarizes the implications of plasticity for retinal disease.

General Organization of the Retina

The retina is a heterocellular (Fig. 1A,B) collection of interacting cellular systems and is assembled from three developmentally distinct neuron-like groups (Table 1). Superclass 1, the sensory neuron phenotype, is a superset of rod and cone photoreceptors and BCs, all characterized by

polarized epithelial forms with apical ciliary-dendritic and basal axonal-exocytotic poles (6). These cells uniquely use high fusion-rate synaptic ribbons as their output elements. Superclass 2, the multipolar neuron phenotype (7), is a superset of ACs, axonal cells (AxCs) and GCs characterized by numerous branching neurites (often separable into dendrites and classical axons) and classical CNS Gray type I and II synapses. Superclass 3 contains the gliaform cell phenotype (7) and the superclass of HCs. Though they are multipolar and may display axons, they do not spike and also express many otherwise uniquely glial attributes. A complete vertebrate retina also requires two traditional classes of glial cells radial Müller's cells (MCs) and astrocytes (AsCs). Mammalian retinas are also unique in expressing retinal vascularization (Fig. 1C). This requires the migration of vascular endothelial phenotypes and pericytes into a permissive retina and the molecular mechanisms of this process remain unknown. Finally, vertebrate retinas contain populations of surveillant microglia (8, 9).

Like other complex CNS assemblies, neuronal populations of the retina are segregated into distinct layers of cell somas (nuclear layers) with interposed layers of syn-

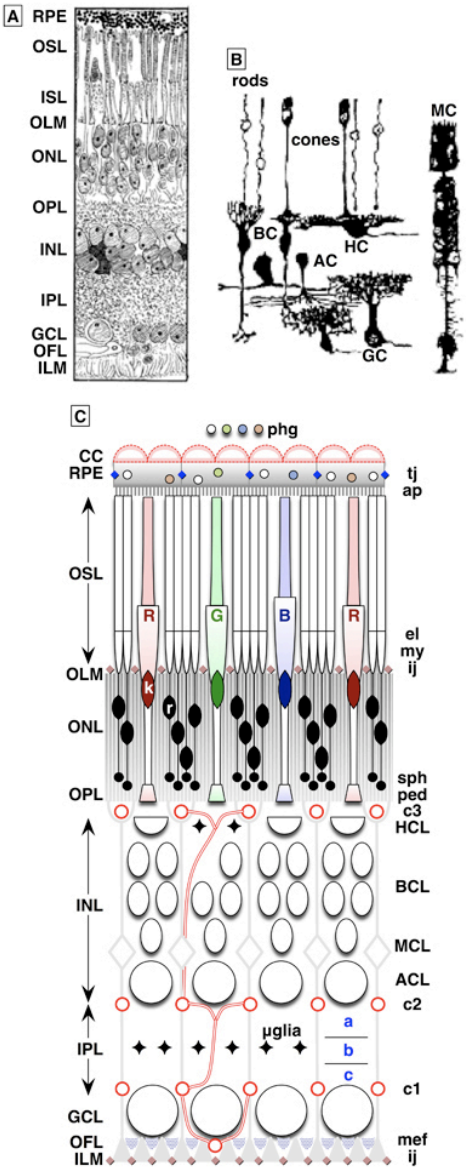

Figure. 1. General organization of the mammalian retina.

A. A classical hand drawing of a vertical section through the retina showing the arrangement of the nuclei of retinal cells into discrete layers. B. Representative Golgi-impregnations of representatives of the major classes of retinal neurons and the principal glial cell, the Muller cell, taken from Ramón y Cajal's (1) drawings of mammalian retinas. (C) A detailed schematic of the relations among photoreceptors, neuronal layers, and the non-neural elements of the retina viewed as a neurovascular unit.

Abbreviations:

RPE: retinal pigmented epithelium, OSL/ISL: outer/inner segment layer, OLM/ILM: outer/inner limiting membrane, ONL/INL: outer/inner nuclear layer, OPL/IPL: outer/inner plexiform layer, k: cone nucleus, r: rod nucleus, R/G/B: LWS:red/LWS:green/SWS1:blue cones, tj/ij: tight/intermediate junctions, AC: amacrine cell, BC: bipolar cell, GC: ganglion cell, HC: horizontal cell, MC: Müller cell, HCL/BCL/MCL/ACL/GCL: HC/BC/MC/AC/GC layer, a/b/c: sublaminas a/b/c, c1/c2/c3 capillary arcades of the GC/AC/HC layers, OFL optic fiber layer, ap apical processes, el ellipsoid, mef Müller cell end feet, my myoid, ped pedicles, phg phagosomes, sph spherules.

Table 1: Classification of Retinal Neurons

Superclass 1 Sensory Neuron Phenotype
1.1 Photoreceptors
1.1.1. Class SWS1 cones
1.1.2. Class LWS cones (R & G variants)
1.1.3. Class RH1 rods
1.2 Bipolar Cells
1.1.1. SWS1 cone selective 1,2 classes
1.1.2. LWS1 cone selective 3 classes
1.1.3 RH1 rod selective - 1 class
1.1.4 All cone selective - 5-6 classes
Superclass 2 Multipolar Neuron Phenotype
2.1 Projection Neurons
2.1.1. Ganglion cells - 15-20 classes
2.1.2. Axonal cells - ? classes
2.2 Local circuit neurons
2.2.1. Lateral ACs 25+ classes, mostly GABAergic
2.2.2. Vertical ACs - 5+ classes, mostly glycinergic
Superclass 3 Gliaform Neurons
2.1 Horizontal cells

Non-neuronal classes: RPE, MCs, AsCs, microglia, vascular endothelia, pericytes

aptic connections (plexiform layers). The outer nuclear layer contains the nuclei of rod and cone photoreceptors embedded in a meshwork of distal MC processes, and constitutes the nuclear zone of the image-forming *sensory retina*. The inner nuclear layer is the distal part of the true *neural retina* and contains four cell groups layered in distal-to-proximal order: HCs, BCs, MCs and ACs (Fig. 1C). The GC layer contains the somas of the CGs, the true projection neurons of the retina, which decode BC signals and and re-code them as spike trains. These packets of coded information are distributed by GC axonal projections to thalamus and midbrain. Interposed between the ONL and INL is a thin outer plexiform layer containing the synaptic output of photoreceptors and the dendrites of BCs and HCs. Interposed between the inner nuclear and ganglion cell laters is a thick inner plexiform layer containing the axonal outflow of BCs, the dendrites of GCs and the dendrites and synaptic output of diverse classes ACs and AxCs. Together, these elements form the basic set of components for vision (Fig. 2).

Photoreceptors form the sensory retina. Their distal ciliary extensions form the light-harvesting outer segment layer in mammals (Fig 3), and their proximal somatic and axonal extensions form the neural interface between photoreceptors and the afferent neural chain to the CNS. There are three classes of photoreceptors: (i) rods , (ii) long-wave system (LWS) cones and (iii) short-wave system 1 (SWS1) cones. Each class displays a distinct morphology as well as visual pigment (Fig. 3), but the full array of genes that confer rod, LWS or SWS1 cone identity remains unknown. Visual pigments (opsins) are GPCRs that bind 11-cis retinaldehyde as their ligand in mammals. Rods alone express the RH1 visual pigment *rhodopsin* that absorbs maximally at 499 nm (VP 499). LWS cones express either red (R) VP 560 or green (G) VP 530, via a yet uncertain semi-stochastic switch (10). There are no known gene expression differences in LWS$_R$ and LWS$_G$ cones other than the visual pigment. Indeed, LWS$_R$ and LWS$_G$ cones are morphologically indistinguishable. Conversely, SWS1 cones differ from LWS cones in subtleties of shape (they are slightly longer and slimmer), connectivity (fewer ribbons) and other gene expression patterns (7). Human or primate SWS1 cones express VP 420 and are also referred to as blue (B) or short-wave (S) cones. Similarly, R cones are also termed L or long-wave cones and G cones termed M mid-wave cones. We will generally use the R, G, B notation as it conforms to the psychophysical color percepts the cones drive.

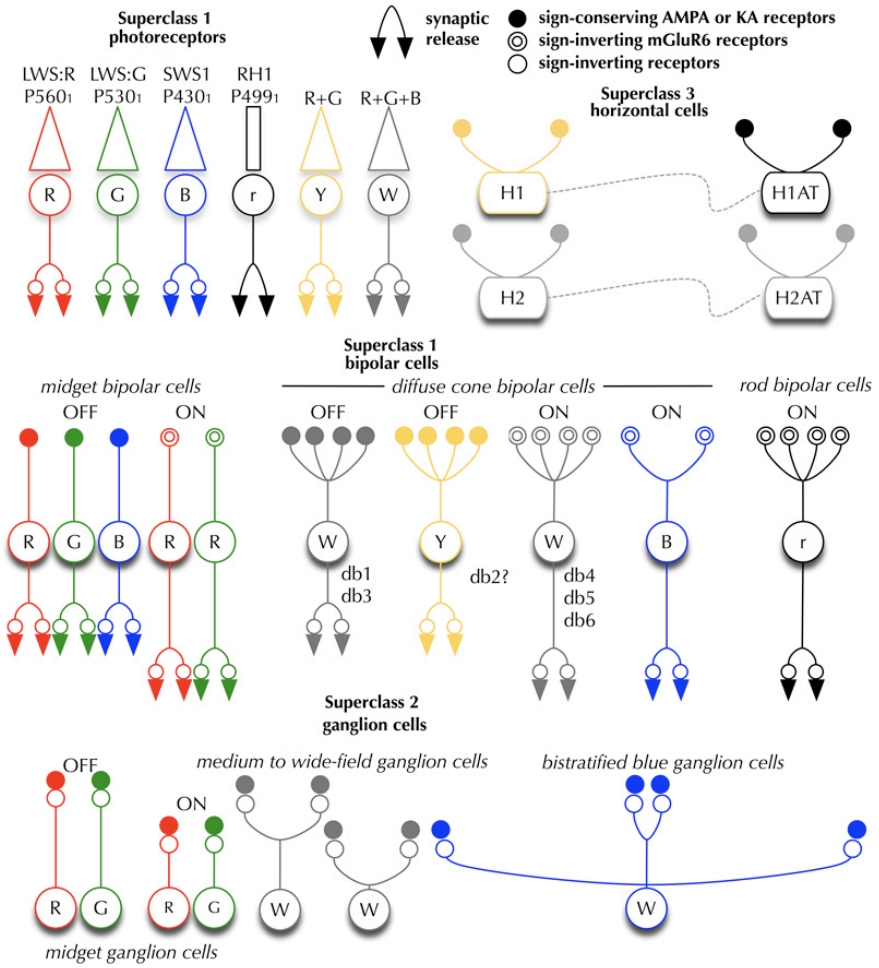

Figure 2. Iconic circuit summary of key primate retinal neurons.

The primate photoreceptors contain three classes: LWS (R and G) cones, SWS1 (B) cones and RH1 rods. Cells that selectively contact LWS cones are labeled Y (yellow) cells. Cells that contact all cones are labeled W (white) cells. BCs contain between 10-15 classes, including midget BCs that selectively contact one cone, diffuse BCs that contact all (db1,3,4,5,6) or perhaps only Y cones (db2), B cone-selective BCs, and rod BCs. In superclass 2, GCs are extremely diverse and range rrom midget GCs to medium to wide field cells. In superclass 3, HCs form at least two classes: H1 cells contact all cones but are Y biased in function; H2 cells contact all cones with stronger, more balanced B-rich inputs. H1ATs receive input from rods, and H2ATs from rods and cones.

The light-driven switch that activates signaling is the absorption of photons by 11-cis retinaldehyde-opsin to form all-trans retinaldehyde-opsin, which activates binding of the ATP-activated form of the G-protein transducin to opsin and triggers a transduction sequence that leads to closure of cation permeant channels on the photoreceptor outer segment. This closure represents a conductance decrease to a cation with a positive reversal potential and is manifest as photoreceptor hyperpolarization. This voltage change directly gates the rate of synaptic glutamate release by photoreceptor terminals. When depolarized in the dark, photoreceptors release maximal amounts of glutamate; when hyperpolarized in light, release is attenuated.

BCs decode photoreceptor glutamate signals and re-code them as their own

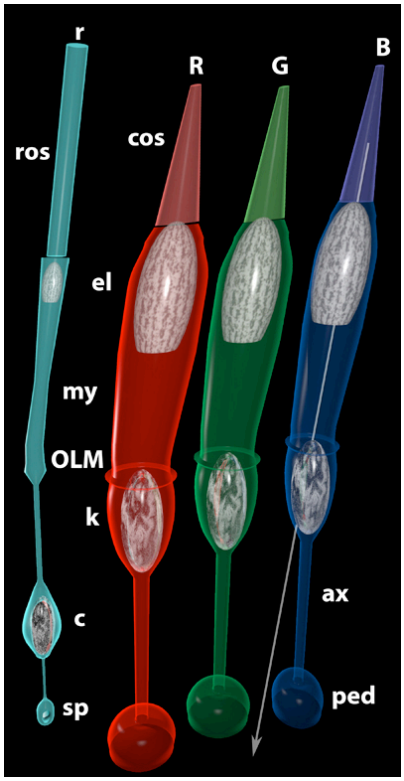

Figure 3. A rendering of primate peripheral cones (R,G,B) and rods (r).

Each photoreceptor has an outer segment coupled (rod: ros, cone: cos) connected to the inner segment by a narrow ciliary neck. The distal-most portion of the inner segment is formed by the ellipsoid (el), a dense mitochondrial pack. The myoid (my) contains the golgi, smooth and rough endoplasmic reticulum and is the protein synthesis zone. The subretinal space and the true neural retina containing the rod (c) and cone (k) nuclei, their axons (ax) and their synapses (rod spherules: sp, cone pedicles, ped) are separated by a layer of intermediate junctions termed the outer limiting membrane (OLM). Beyond the OLM, photoreceptors act as fiber optics and they are tilted to orient their acceptance apertures toward the optical nodal point of the eye (arrow).

voltage-driven glutamatergic synaptic outputs (reviewed in reference 3). Generic synaptic transfers (→) in retinal networks are classified as sign-conserving (>) or sign-inverting ($>_i$). Sign-conserving synapses nominally copy the voltage patterns of the presynaptic cell to the postsynaptic cell. Sign-inverting synapses nominally invert those patterns. Such synapses also possess differences in kinetics and amplification based on their molecular targets. All vertical channel (rod, cone, BC) synapses use glutamate as their transmitter, provide high amplification (greater than 1), and most are sign-conserving. Thus the cone > HC synapse is a quintessential sign-conserving synapse in which HCs mirror the behavior of cones through the readout of glutamate fluctuations by ionotropic glutamate receptors (iGluRs) of the AMPA type: When cones hyperpolarize to light, so do HCs. There are two kinds of BCs: OFF and ON. Cones drive OFF BCs via high gain sign-conserving AMPA or kainate (KA) IGluRs. One of the most unique synapses in the CNS is the high-gain, glutamatergic, sign-inverting synapses between photoreceptors and ON BCs, mediated by a metabotropic glutamate-binding GPCR known as mGluR6. This special high-gain, inverting transition will be symbolized $>_m$.

The fundamental glutamatergic signal flow of photoreceptors → BCs → GCs → LGN neurons → cortex in mammals (a prototypical CNS projection chain) is also shaped by sign-inverting, low-amplification (gain less than 1) feedback and feedforward micronetworks at every synaptic transfer. Most of these feedback / feedforward events in the inner plexiform layer are mediated by classical inhibitory transmitters: 4-aminobutyrate (GABA, γ) and glycine (gly). In the outer plexiform layer, the molecular mechanisms of sign-inverting feedback is unknown, but powerful cone ⇄ HC feedback networks predominate.

Non-neural cells also play a major role in control retinal signaling, though these mechanisms are largely beyond the scope of this chapter. First, as schematized in Fig. 1, the entire retina is sealed distally from

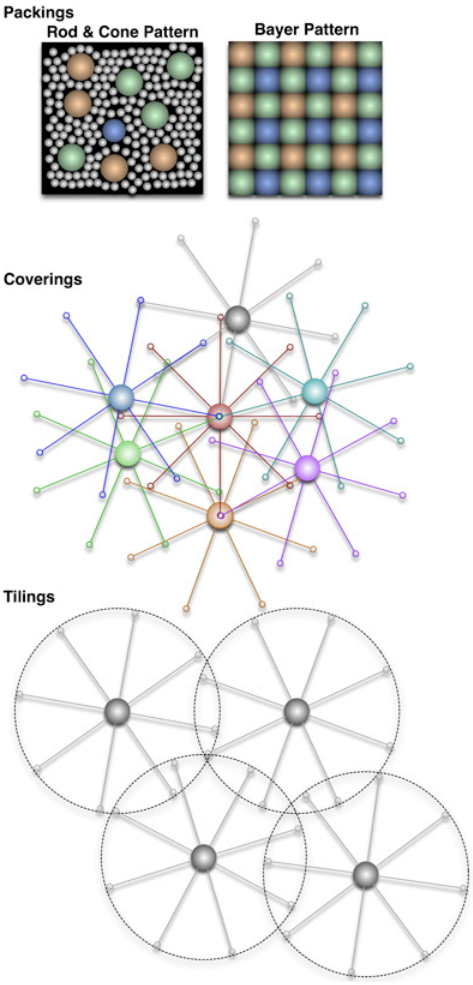

Figure 4. Patterns of retinal cells.

Packings: rods and cones form disorderly but space-filling packings, while the Bayer Pattern used in digital cameras is precise by design. Coverings: ACs of any one class overlap their processes to cover visual space. Tilings: GCs of any one class capture spatial domains to tile the retina without significant overlap. © Robert E. Marc, 2008.

the choroidal vascular compartment by the tight-junctions of the retinal pigmented epithelium (RPE) cell layer and internally mostly by the intermediate junctions of MC processes ensheathing the vascular endothelium (11). In most mammals, three capillary arcades emerge from the vitreal vessels of the ophthalmic artery: the first (c1) branches at the interface between the GC and inner plexiform layers; the second (c2) at the interface between the AC and inner plexiform layers; and the third (c3) exactly at the level of the HCs cells in the outer plexiform layer. There are some important exceptions. Like non-mammalians, retinas of lagomorph mammals (rabbits and hares) are avascular. Order Sciuridae (squirrels) lack the c3 arcade. Importantly, the blood-retinal barrier in arcades c1 and c2 are provided almost exclusively by MCs, whereas HCs and MCs cells form roughly equal contact zones in the OPL at arcade c3 in tree shrews (12). Whether this is generic for primates has not yet been established, but suggests that HCs have glial-like endothelial recognition systems. This is intriguing for two reasons. First, only mammals display retinal vascularization and recent discoveries of secreted VEGF inhibitors that maintain corneal clarity (13) suggests that similar molecular mechanisms may have played a role in evolutionary regulation of retinal vascularization. Second, the tolerance of the mammalian retina for vascular cells also invites pathological over-invasion, such as in neovascular macular degeneration. A recently characterized form of neovascularization apparently arises from arcade c3 and is termed retinal angiomatous proliferation (RAP) (14). It is plausible that RAP involves loss or modulation of HC. AsCs reside in the layer of optic nerve fibers and sometimes around retinal capillaries in arcade c1.

RETINAL PATTERNING

Retinal photoreceptors convert a photon-based image into a mixed array of photoreceptors generating primary photocurrents transformed into synaptic drive (15). We can think of this drive as a synaptic image. The cone mosaic of humans and primates is patterned (Fig. 4) in a manner

roughly analogous to the Bayer pattern of digital color CCD arrays (16, 17). While not tiled like non-mammalian cone arrays (18) and nearly random in organization, the cones of primates are differentially expressed (17, 19) so that B cones comprise a minority: about 7% of the human mosaic (20). The remaining cones are a mix of R and G, the ratio varying widely across individuals, ranging from a high of 16.5:1 to about 1:1 in males, and 0.37:1 in some females (21). In primates, the photoreceptor layer is dominated by rods *except* in the central 2 degrees of visual angle, where cone density rapidly rises to a sharp peak at 160,000 cones/ mm^2 (Fig. 5) and the rod density drops to zero in the foveola (22), a region about 0.25 degrees in diameter. In the periphery (beyond 20 degrees), the cone density drops to 5000 cones/mm^2. Importantly, the cone inner segments (the light capture compartment) become proportionally larger in the periphery, increase diameter from about 2 μm in the foveola to 7-8 μm beyond 20 degrees. Thus the coverage of image space by cones smoothly decreases from 100% to no less than 30%. This is quite different from rodent retinas where the cone density may be higher (> 10,000 cones/mm^2) than peripheral primate retina but image coverage never exceeds 3% (23). Cone density is less important than the coverage.

Neurons are also patterned on global and local scales (24, 25). Local patterns are termed mosaics (Fig. 5) and each cell class possesses its own own portion of a segmented synaptic image. The functional attributes of these mosaics in forming synaptic images are determined by several features of individual cells: their abundance, regularity of spacing, dendritic overlap and synaptic density. Dendritic overlap and abundance are often combined into a dimensionless coverage factor (CF): the product of the projected planar area subtended by the dendritic arbor of an average cell (mm^2/cell) in the class and its spatial density (cells/mm^2). Three distinct pattern classes (15) or mosaics are found in the vertebrate retina and are characterized by their overlap features. *Packings* are mosaics with no overlaps allowed, though there may be gaps. Photoreceptors form packings with CF < 1. In other words, each point in visual space is sampled by only one photoreceptor, which necessary excludes all other photoreceptor classes. *Coverings* are mosaics that allow no gaps, but permit overlap. ACs overlap their dendritic arbors to form coverings with CF >>1. Perfect *tilings* are idealizations that admit neither gaps nor overlaps and CF = 1. The classes of the GC cohort roughly approximate tilings. Thus the initial synaptic image is fractionated into rod, LWS_R, LWS_G and $SWS1_B$ packings and these collections partially smoothed by tiles of each GC class, with further smoothing by high-coverage factor ACs and HCs. Paradoxically, the dendritic arbors of HC have small overlap compared to ACs and more resemble CNS astrocytes. However, a powerful mechanism generates a high physiological coverage factor: connexin-based coupling. This will be addressed in detail later.

Local patterning is a measure of the spatial precision of a class. Spacing in a class can be statistically orderly, ranging from nearly perfect crystalline patterns such as cone (26) and BC patterns in fish eyes (27), to random as shown by AxC classes such as interplexiform cells (28). For the latter and for neurons that have high coverage factors, the spacing is measured as the distance between somas, which is a rough gauge of the center of mass for a mosaic

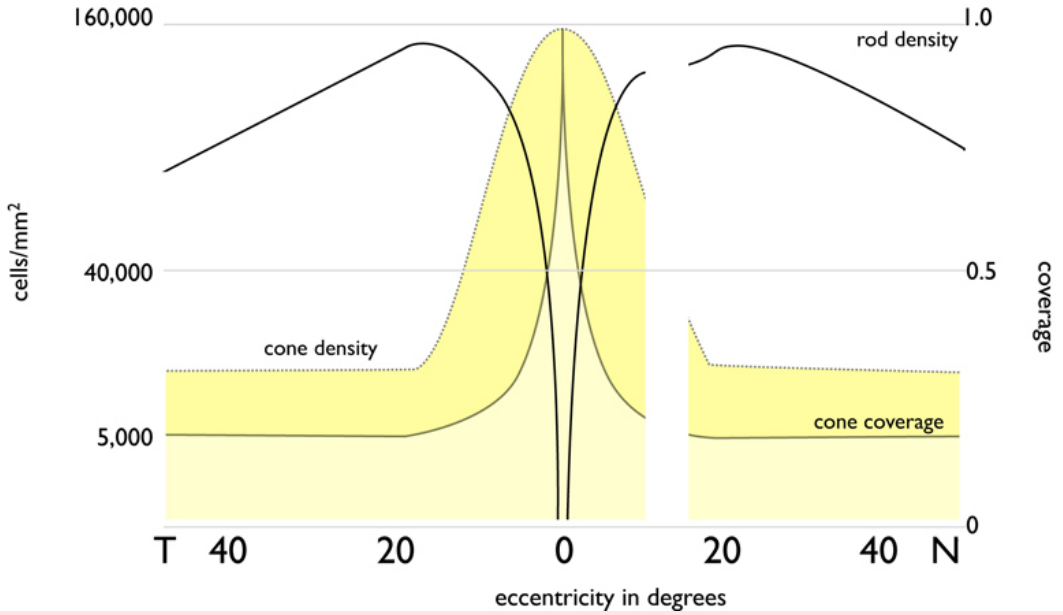

Figure 5. Photoreceptor distributions in the human eye.

Curves are plotted on a square root scale (ordinate) versus eccentricity (abscissa). Rod density (solid black line) peaks at about 150,000 cells/mm² at 20 degrees from the fovea. Cone density (dotted line) peaks at about 160,000-200,000 cells/mm² at the foveola. Replotted from Curcio CA, Sloan KR, Kalina RE, *et al.* Human photoreceptor topography. *J Comp Neurol*, 1990;292:497-523. The faction of light captured by cones, coine coverage (solid colored line) is shown on the right ordinate, and drops from 1 in the foveola to about 0.3 in the periphery.

element. The precision of spacing is gauged several ways, the most common being the non-dimensional conformity ratio (CR)(25, 29), also known as the regularity index (24): the ratio of the mean minimum distance between cells to its standard deviation. Thus highly precise patterns with little spacing variability have large CR values and random ones have CR of about 1. Normally, CRs of mammalian retinal neurons rarely exceed 4, while non-mammalian fish photoreceptor CRs can approach 30. Such high precision in patterning is likely closely associated with velocity detection in more complex visual environments than experienced by mammals.

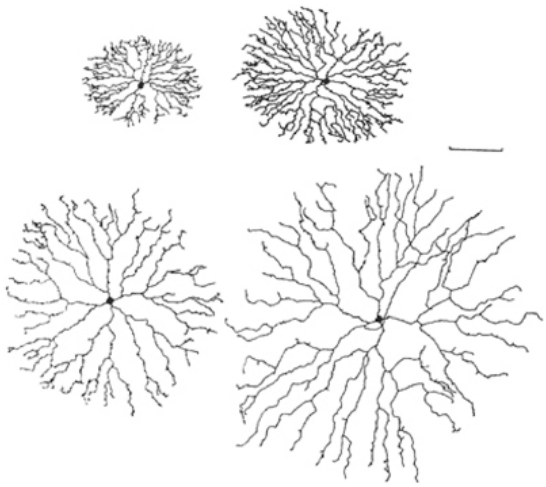

Figure 6. Camera lucida drawings of four starburst ACs from the rabbit retina, located at increasing distance from the center of the eye. The basic shape of the cell remains the same, but the size increases. Marker bar is 100 µm. The numbers indicate the relative position of the drawn cell in the series. (Tauchi M, Masland RH: The shape and arrangement of the cholinergic neurons in the rabbit retina. Proc R Soc Lond B223:101, 1984, with permission of the authors)

Global patterning rules impact retinal function as cell abundance can vary with eccentricity, forming central zones with class mixture specialized for acuity and

chromatic processing (7, 25). In the humans, the retina possesses a rod-free declivity where neuronal cell bodies (intense Rayliegh scatterers) are displaced in an aster pattern around the foveola and cone diameters decrease to about 2.5 um, achieving densities of 160,000 cones/mm2 (22). The peak rod density is found at about 20 degrees parafoveally in nasal and temporal retinas (Fig. 5). Thus, cone-selective BCs and GCs are at their highest densities in central retina, while rod-specific neurons are concentrated in an annulus around the fovea. Other highly visual mammals such as cat and rabbit lack optically optimized foveas but still display elevated concentrations of cones in central regions in which cones are found at a higher density, though lower than in primates. A correlate of this density gradient is that, like cones, most neurons are smaller in the central retina (packed more densely) and larger in the periphery (25), including HCs, rod BCs (30), GCs of the primate retina (31), and ACs (32). Figure 6 illustrates the variation in starburst AC size with increasing eccentricity. Correspondingly, larger dendritic arbors provide larger physiological receptive field sizes (33)and decreases in the resolving power in peripheral retina.

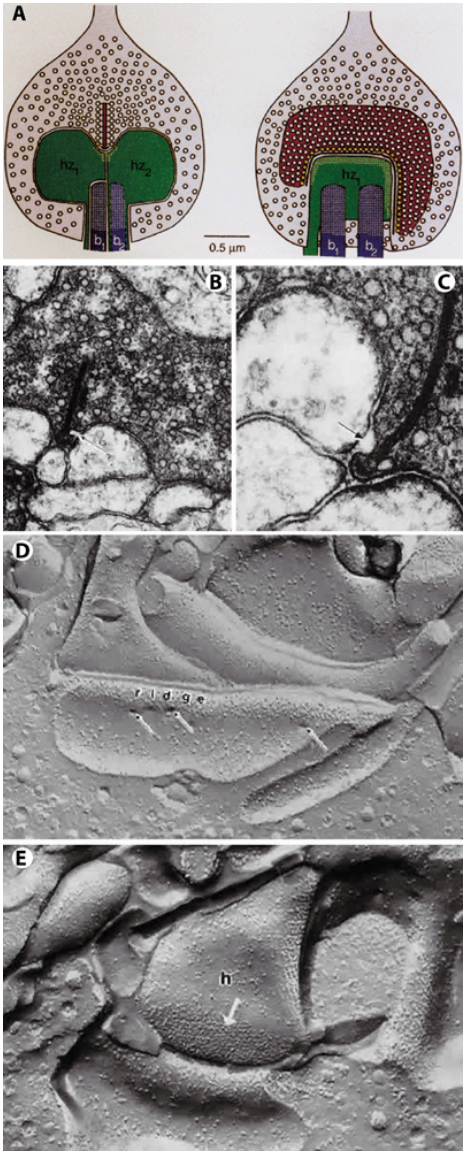

SYNAPSES AND GAP JUNCTIONS IN THE RETINA

Each neuron *decodes* upstream visual signals via distinctive sets of receptors for specific neurotransmitters or molecular sensors for other chemical signals, such as nitric oxide (3). Generically, each neuron

Figure 7. The ultrastructure of rod synaptic ribbons.

A. Schematic of a rod photoreceptor terminal in the mammalian retina. The left drawing is perpendicular to the ribbon, the right drawing parallel to the ribbon. Presynaptically, a long active zone docks about 130 vesicles (yellow) and the extensive ribbon tethers about 770 vesicles. Postsynaptically, four processes (two HC and two BC [b]) occupy the invagination; the HC receptors (white speckling) arch parallel to the active zone and thus always lie near (16 nm) the docking sites; the BC receptors (white speckling distributed over entire surface) lie far (130 to 640 nm) from the docking sites. The mouth of the invagination is exaggerated because parts of the rod were cut away for clarity. (Drawing and description from Rao-Mirotznik R, Harkins A, Buchsbaum G, Sterling P: Mammalian rod terminal: architecture of a binary synapse. Neuron 14:561, 1995, with permission of the authors and Cell Press). B, C. Ribbon synapses in rod photoreceptor bases of the Xenopus retina. Note the fusion of a synaptic vesicle with the rod membrane adjacent to the synaptic ribbon (arrows). (A, × 72,000; B, × 120,000; courtesy of P. Witkovsky and C.C. Powell). D. A freeze-fracture view of the photoreceptor synaptic ridge characterized by a densely packed array of P-face particles (ridge). Adjacent to the ridge are three vesicle fusion sites (arrows). (× 100,000) E. A HC dendrite (h) showing a dense array of P-face particles (arrow), which may represent glutamate receptors (× 115,000). (Data of A.R. Nagy and P. Witkovsky)

Table 2: Major retinal neurotransmitter systems

Molecule	Sources	Targets	Receptor Class	Receptor	Signaling Modes
glutamate	rods, cones	HCs	iGluR	AMPA	Cat, High-gain, sign-conserving
		OFF BCs	iGluR	AMPA, KA	Cat, High-gain, sign-conserving
		ON BCs	III mGluR	mGluR6	Cat, High-gain, sign-inverting
	BCs	ACs, GCs	iGluR	AMPA, NMDA	Cat, High-gain, sign-conserving
			I, II mGluR	mGluR1,2,3,5	Modulation of Ca^{2+} levels
		MCs	iGluR	NMDA	Cat, High-gain, sign-conserving
	GCs	CNS	iGluR	AMPA, NMDA	Cat, High-gain, sign-conserving
GABA	ACs	BCs	ionotropic	$GABA_C$	An, Low-gain, sign-inverting
		ACs, GCs	ionotropic	$GABA_A$	An, Low-gain, sign-inverting
		BCs, GCs	metabotropic	$GABA_B$	Ca^{2+}, K^+ channel modulation
glycine	ACs	BCs, ACs, GCs	ionotropic	glyRs	An, Low-gain, sign-inverting
ACh	ACs	ACs, GCs	ionotropic	nAChRs	Cat, High-gain, sign-conserving
		ACs, GCs	metabotropic	mAChRs	K^+ channel modulation
dopamine	AxCs	all cells	metabotropic	D1	typically cAMP level increase
				D2	typically cAMP level decrease
NO	ACs	all cells?	metabotropic	soluble GuCyc	typically cGMP level increase

Abbreviations: Cat cationic; An anionic; I, II, III major mGluR group; glyR glycine receptor; ACh acetylcholine; nAChR nicotinic ACh receptor; mAChR muscarinic ACh receptor; NO nitric oxide; GuCyc guanyl cyclase

decodes an array of incoming molecular signals into its voltage responses and encodes those into its own neurotransmitter release patterns. For example, photoreceptors decode the rate of photons captured by VPs as photovoltages and *encode* those photovoltages as time-varying synaptic glutamate release; at the next element in the chain, BCs decode the rate of glutamate molecules released by photoreceptors as synaptic currents, summed as cellular voltage responses, and encode their own synaptic glutamate release.

Most synapses in the vertebrate retina are *fast*: presynaptic encoding / postsynaptic decoding pairings that mediate millisecond-scale signaling. Fast synapses are assembled in one of two architectures: ribbon and conventional. High-performance glutamatergic ribbon synapses (Fig. 7-9) of photoreceptors and BCs contain large vesicle pools and display sustained vesicle fusion rates approaching 1000 vesicles/second (34). Conventional fast γ, gly and cholinergic (ACh) synapses made by AC cells involve small vesicle clusters, limited fusion rates and short du-

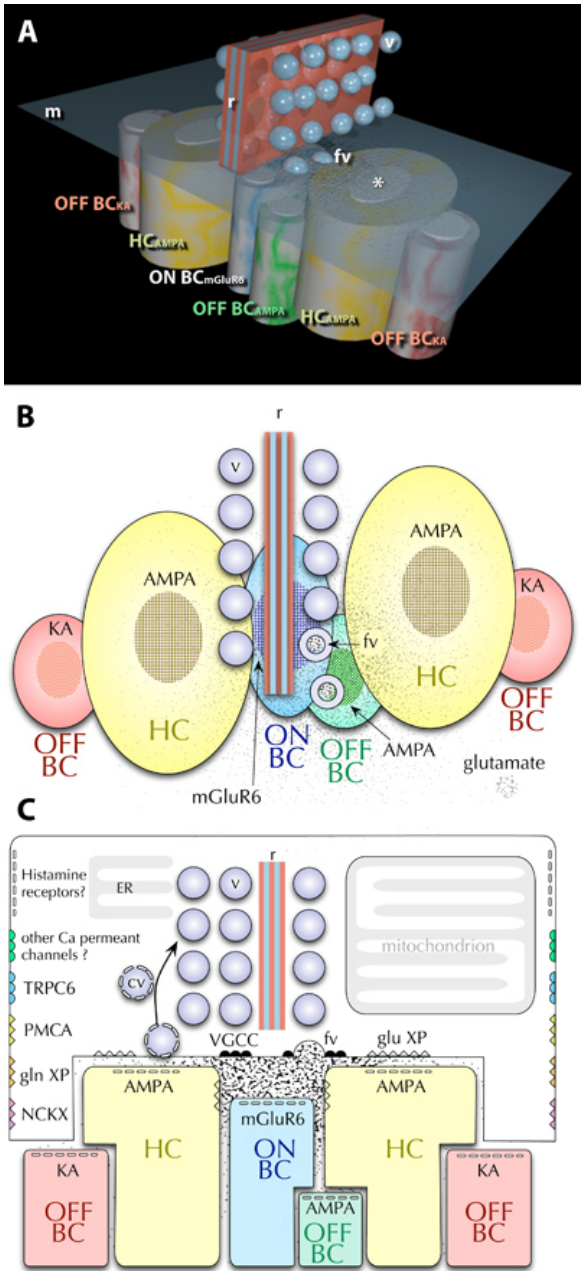

Figure 8. The ultrastructure of cone synaptic ribbons.

Each cone contains 20-50 synaptic ribbons and each ribbon has a specific signaling architecture. A. A flattened cone ribbon complex viewed as a transparent rendering. The synaptic ribbon (r) aggregates glutamate-filled vesicles (v) for Ca^{2+}-mediated fusion (fv) with the cone membrane (m). This releases a cloud of glutamate molecules (*) into the synaptic cleft. Dendrites of target cells are stereotypically positioned opposite the ribbon. Beneath the ribbon but displaced from it are the dendrites of ON BCs expressing mGluR6 receptors and OFF BCs expressing AMPA receptors. Flanking the ribbon close to the membrane are large HC dendrites expressing patches of AMPA receptors. Furthest away (about 500-1000 nm) are the dendrites of OFF BCs expressing KA receptors. B. A projection viewed from inside the cone through the membrane showing that glutamate released (stippling) from fusion vesicles (fv) form a gradient from high to low concentration. C. A vertical projection showing the same glutamate gradient and additional complexities of the cone pedicle including the endoplasmic reticulum (ER), VGCCs, glutamate transporters (glutamate XP), Na^{+}-Ca^{2+}-K^{+}- exchangers (NCKX), plasma membrane Ca^{2+}- transporters (PMCA), TRPC6 channels (TRPC6), perhaps other Na^{+}-permeant channels and histamine receptors. © Robert E. Marc, 2008.

rations of release (35). Inhibitory GABA-releasing synapses represent the majority of synapses in the retina (Fig. 10), likely due to the need to control the powerful synaptic output of BCs. Both ribbon and conventional synapses are focal in action and represent a unidirectional transfer of information at a pair of processes in a synaptic network. A variant of the conventional synapse is the *en passant* or non-paired form in which dopamine or peptides are released into the extracellular space via volume conduction to modulate cells in a global rather than discrete mode. A detailed review of transmitters and receptors in the vertebrate retina has recently been published (3) and is summarized in Table 2.

An important feature of synaptic transmission is its regulation by voltage-gated calcium (Ca^{2+}) currents. An array of low-voltage threshold (L-type) Ca^{2+} channels are localized to synapses near synaptic vesicle docking proteins and participate in converting cell voltage into neurotransmitter release by controlling vesicle fusion rates. When these channels open, thin domain of cytoplasm subjacent to the

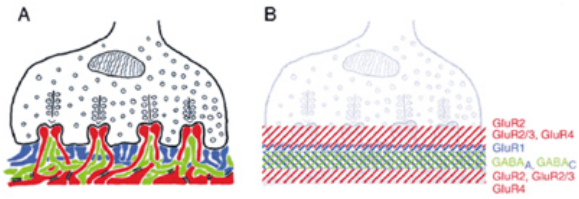

Figure 9. The glutamate receptor architecture of the mammalian cone pedicle.

A. Schematic drawing of the cone pedicle with the dendrites of horizontal (red), ON cone bipolar (green), and OFF cone bipolar (blue) cells. The desmosome-like junctions are indicated by the black double lines. B. Drawing of the cone pedicle and the precisely laminated expression of glutamate receptors and GABA receptors. (Haverkamp S, Grunert U, Wässle H: The cone pedicle, a complex synapse in the retina. Neuron 27:85, 2000, with permission of the authors and Cell Press)

membrane experiences a rapid, large increase in $[Ca^{2+}]_i$ (10 to 100 μM), 3-4 higher than basal levels (36). In the remainder of the presynaptic terminal, however, $[Ca^{2+}]_i$ does not rise as high because of extensive buffering via calcium-binding proteins, export pumps, and sequestration in endoplasmic reticulum and mitochondria compartments (37). The dynamics of these compartments are clearly critical components of synaptic signaling and the molecular partners are only now being clarified (38). For example, the loss of photoreceptor-specific Ca channels (Cacna1F) in the *nob2* ("no-b-wave") mouse renders rods unable to signal, thus creating a synaptic form of congenital stationary night blindness (39).

A second intercellular mechanism allows direct electrical signal sharing across cell pairs: electrical coupling mediated by gap junctions . Gap junctions (sometimes called electrical synapses) are assemblies of transmembrane proteins known as connexins (40-42). Connexins self-assemble into hexameric connexons resembling

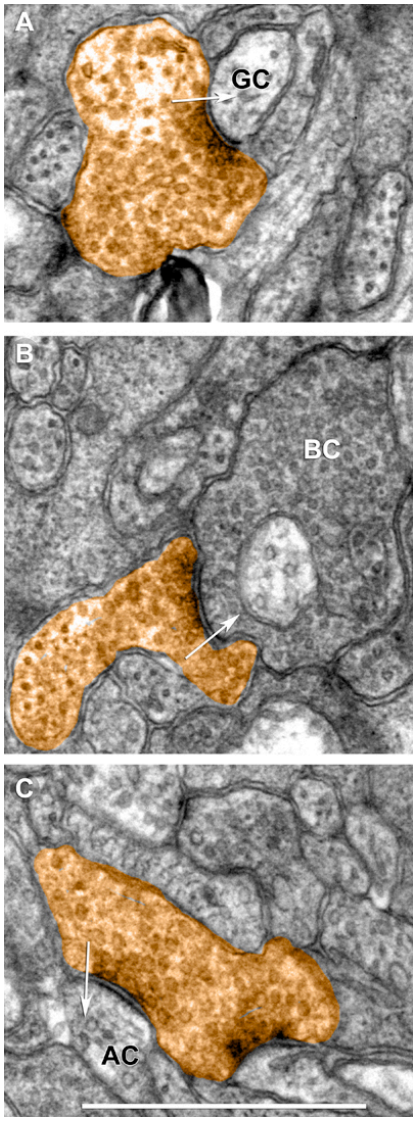

Figure 10. Conventional GABAergic AC synapses in the mammalian retina.

AC presynaptic terminals (orange) with vesicle accumulatiosn near dense plasma membrane profiles targeting (A) GCs, (B) BCs and (C) other ACs. The synaptic polarity is indicated by the arrow. Scale, 500 nm. Marc, Watt, Jones and Anderson, unpublished data.

transmembrane tunnels with pore sizes up to 2 nm in diameter (Fig. 11). Pairs of connexons in adjacent cells align their pores to form transcellular channels and large rafts of connexons, like parallel resistors, allow large transcellular currents to flow.

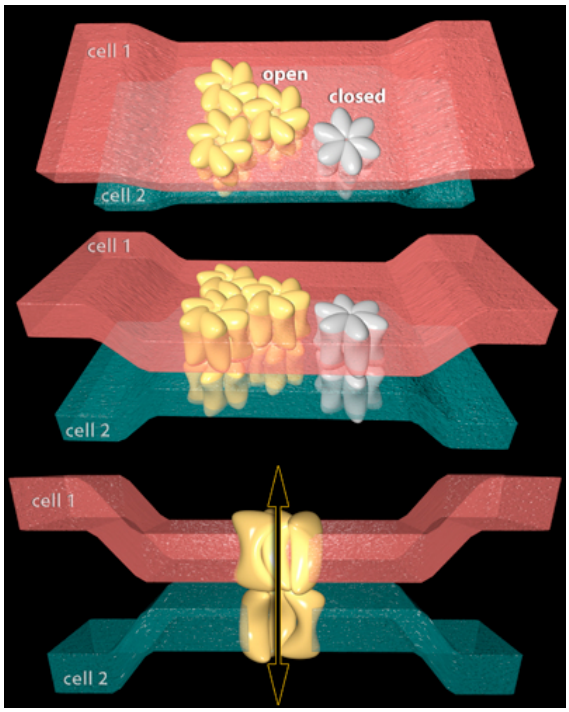

Figure 11. Scale renderings of connexons forming gap junctions between cells.

Each connexon is a hexamer of connexins and the tilt of the subunits determines whether the junctions are open or closed. The normal extracellular gap between cells is roughly 10 nm, but when connexons in adjecent cells bind, the pull the membranes close to within 2 nm of other forming the so-called gap. When aligned, gap junctions form a diffusion pore of roughly 2 nm diameter between the cells.

Connexons can allow direct flow of molecules up to 1000 Kd between cells. The key differences between unidirectional synaptic and bidirectional gap junction signaling is that synapses require energy, and can amplify and control the polarity and waveforms of signals, while gap junctions generally cannot. Gap junctions provide a low-energy, efficient way of fanning out signals from a neuron to selected partners within or across cell classes. For example, HCs tend to be highly coupled to each other, and from the standpoint of electrical current spread, a patch of adjacent HCs acts like a single large cell.

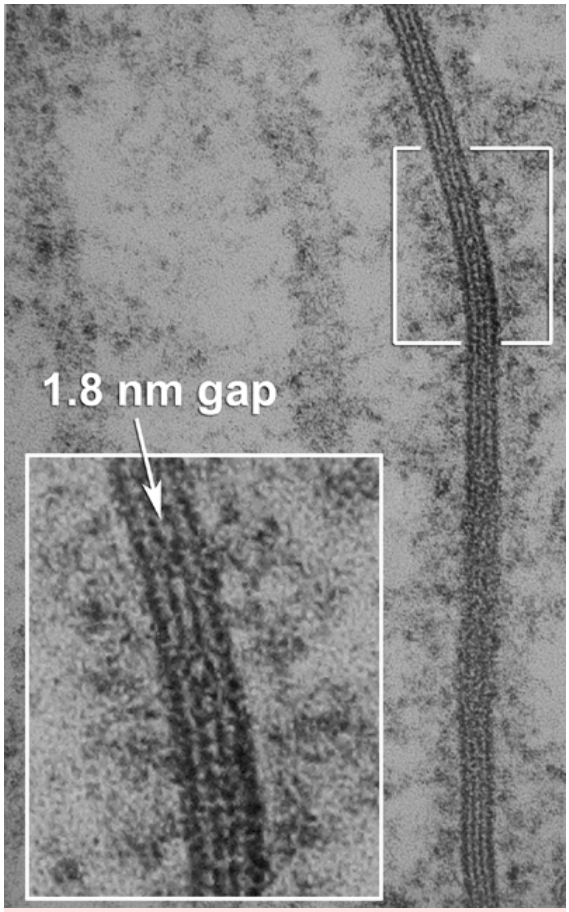

Figure 12. Electron microscopy of a large gap junction between two AC dendrites in the retina.

A well-aligned region shows the heptalaminar pattern of a true gap junction. The enlargement marks the 2 nm extracellular gap. Scanned from original data negatives of Marc, Muller and Liu.

Gap junctions vary in size, type and coupling efficacy (43). There are many vertebrate connexin (Cx) genes. The most important in mammals are Cx36, Cx45, Cx50 and Cx57 (42). Cx36 predominantly mediates coupling between photoreceptors (44), between some sets of ACs cells (45), and in varied mixtures with Cx45 (or Cx45 alone)(46), between some ACs and BCs. Gap junctions between photoreceptors are often small, with connexin patches 100 nm wide (42, 47), while HCs cells are coupled by gap junctions up to 5000 nm. As connexon densities are similar across

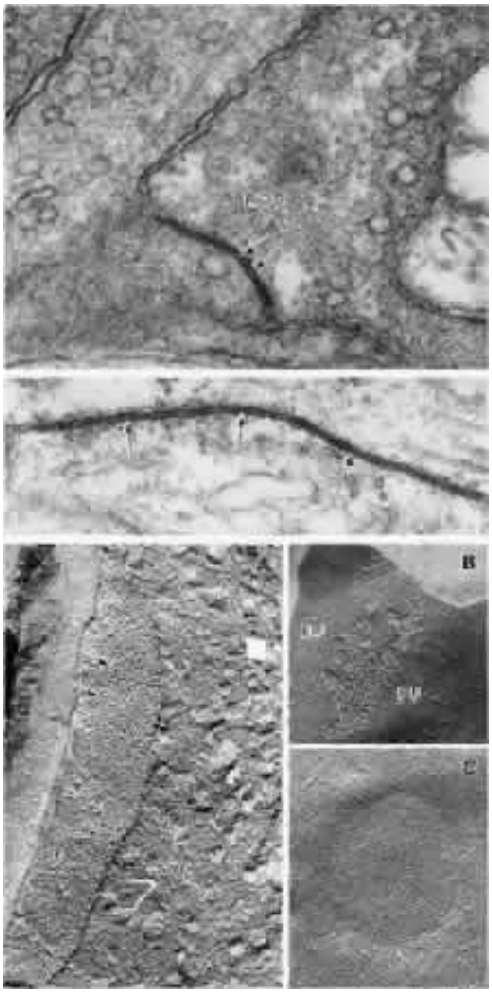

Figure 13. Gap junctions in retinal photoreceptors and HCs.

Part 1. Gap junctions viewed by transmission electron microscopy. Top. A gap junction (arrows) between a rod base (ROD) and a basal process emitted by a neighboring rod (left) in the Xenopus retina (× 180,000). Bottom. An extensive gap junction (arrows) between two HC axons in a Xenopus retina (× 216,000; data of P. Witkovsky and C.C. Powell). Part 2. Gap junctions viewed by freeze fracture. A. Gap junction (large arrows) on the protoplasmic face (PF) of the photoreceptor base in the Xenopus retina. At right the receptor cytoplasm is seen in cross fracture; synaptic vesicles (SV) are indicated by small arrows (× 109,500). B. Gap junction on the photoreceptor membrane in the Xenopus retina. The fracture plane passed through the junction, revealing both the protoplasmic face (PF), bearing particles, and the external face (EF), bearing pits associated with the gap junction (× 127,750). C. HC gap junction in the *Xenopus* retina. The external membrane face contains a plaque of E-face pits (× 27,750; data of A. Nagy and P. Witkovsky).

cell classes (about 5,000/μm2), larger gap junctions carry more current. Importantly, gap junctions can also be modulated, opened or close in response to a variety of signals. Many types of retinal neurons are electrically coupled through gap junctions (Fig. 12,13). The coupling may be strong, as in the homocellular coupling of HCs (48), AII ACs(49), or weak, as has been shown for cones (42) or CGs(50).

PHOTORECEPTOR SYNAPTIC TERMINALS

Rods and cones drive massive amounts of synaptic glutamate release in the OPL via their synaptic terminals (51). The short axons of rods enlarge into spherules or synaptic endings about 2-3 μm in diameter (52). In the perifovea (≈ 20°) they form a layer of terminals 2-3 deep just distal to the of layer cone pedicles that borders the OPL. Each spherule contains thousands of synaptic vesicles, one or two curved synaptic ribbons forming a rapidly releasable vesicle pool (53) near the vesicle fusion sites of the spherule presynaptic membrane, and one mitochondrion (54). Glutamate liberated into the synaptic cleft by vesicle fusion is detected by two to four rod BC dendrites and one to four HC axon terminal processes (55). Cone synaptic terminals, called pedicles because of their pediment-like shape, enlarge from their axon to a base over 5 um in width. Pedicles contain many thousands of vesicles, over 50 synaptic ribbons and contact a vast array of targets, perhaps numbering over 100 dendrites from 8-12 types of cells (56).

Photoreceptors tonically release glutamate when depolarized, decreasing the release rate upon hyperpolarization in light (3). In the dark, photoreceptors are relatively depolarized, and their synaptic Ca^{2+}

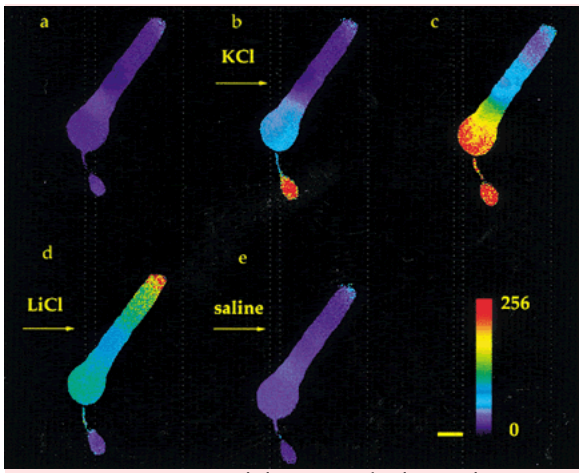

Figure 14. Spatiotemporal dynamics of calcium changes in a rod photoreceptor.

Sequential images of $[Ca^{2+}]i$ changes were recorded from a Fura 2-loaded rod. Between (a) and (b) the rod was superfused with high KCl. The images in (b) and (c) were captured 3 and 21 seconds after KCl application, respectively. The image in (d) was captured 15 seconds after KCl was replaced by LiCl. The image in (e) was captured 7 seconds after the return to control saline. These images show that KCl-evoked increases in $[Ca^{2+}]i$ occurred most rapidly in the synaptic terminal region and then in the basal region of the inner segment. In LiCl, the inner segment and synaptic terminal returned to baseline while $[Ca^{2+}]i$ in the outer segment rose, most notably at the tip. The pseudocolor scale representing the 256 gray levels of the 340/380 ratios is shown on the bottom; red indicates the largest changes. Scale bar, 10 µm. (Adapted from Krizaj, Copenhagen: Neuron 21:249, 1998, with permission of the authors and Cell Press)

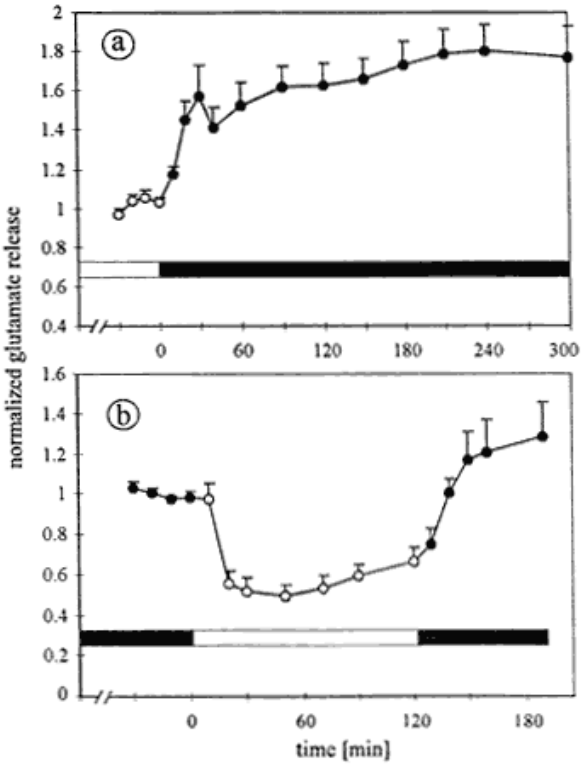

Fig. 15. Dependence of glutamate release on light and dark adaptation.

(a) Xenopus eyecups were treated to remove neural layers, leaving a layer of intact photoreceptors. These "reduced" retinas were maintained for 5 hours in white light, then dark-adapted for 5 hours. Dark and light periods are indicated by the horizontal bar. Each data point represents the glutamate content of 10-minute samples of superfusate (n = 12, mean ± SE). Data are normalized to the average of the light samples. Glutamate release increased markedly within the first 30 minutes of dark adaptation and slightly within the subsequent 4.5 hours. (b) Reduced retinas were dark-adapted overnight, stimulated by white light for 2 hours, then dark-adapted for 1 hour (n = 7). Data are normalized to the average of the first four dark samples. White light reduced release by about 50%. When the light was extinguished, the release rate increased about twofold. (Schmitz Y, Witkovsky P: Glutamate release by the intact light-responsive photoreceptor layer of the Xenopus retina. J Neurosci Meth 68:55, 1996, with permission of the authors and Elsevier Science B.V.)

channels have a higher probability of being open (57), permitting a greater influx of Ca^{2+}, greater vesicle fusion rates and high glutamate release (Fig. 14). Light-evoked hyperpolarization of photoreceptors triggers graded closure of calcium channels, proportional to light intensity, and reduced Ca^{2+} entry slows glutamate release, as illustrated in Figure 15. Voltage-gated Ca^{2+} channels in cones (Cacna 4.1) are concentrated in the synaptic region (58, 59). Calcium export pumps (PMCA2 in cones) are located in bands distal to the vesicle fusion zones and nearer the mitochondria, while Ca^{2+}-Na^{+}-K^{+} exchangers for Ca^{2+} are near the base of the pedicle (60). Their roles are to clear the cytoplasm of excess Ca^{2+}. Further, Ca^{2+}-sequestering sites such as the endoplasmic reticulum, mitochondria and Ca^{2+} binding proteins also regulate the basal Ca^{2+} concentration of the synapse. A major aspect of cones is their ability to adapt to bright lights, which means restoring synaptic Ca^{2+} to dark levels. Major new discoveries in presynaptic Ca^{2+} regu-

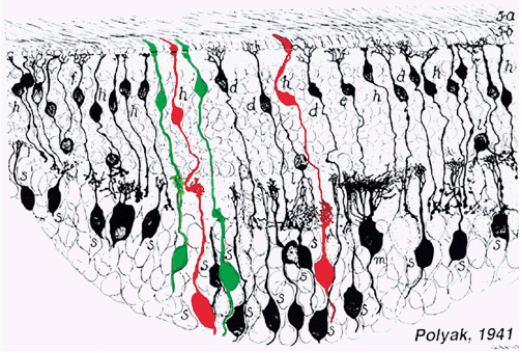

Figure 16. The midget pathways of the primate retina.

The drawing in black is taken from Polyak S: The Retina. Chicago, University of Chicago Press, 1941. The cells drawn in red and green are BCs and midget ganglion cells connecting to L and M cones, respectively. The cone synaptic bases are indicated at top. Each cone type connects to two midget BCs, one of which makes invaginating contacts and ends in the proximal portion of the inner plexiform layer; the other makes basal contacts with cones and ends in the distal portion of the inner plexiform layer. In functional terms, these are, respectively, ON- and OFF-center BCs, which contact ON- and OFF-center midget ganglion cells. (Drawing courtesy of Dr. Helga Kolb)

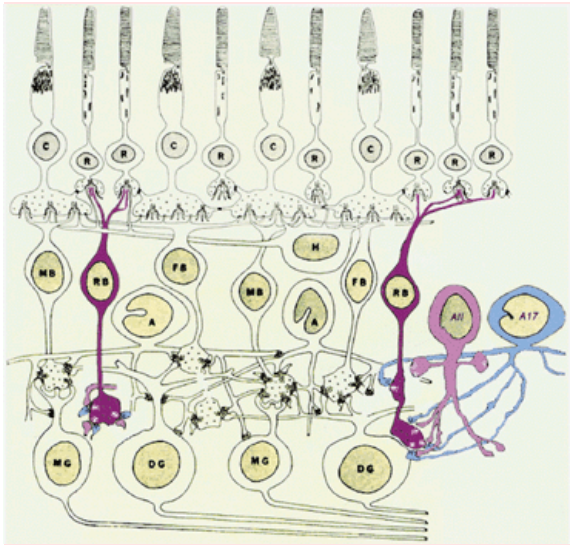

Figure 17. The rod BC pathway of the mammalian retina.

Rod BCs (RB) contact multiple rod photoreceptors (R) in the outer retina. Their axon terminals end in the ON zone of the inner plexiform layer in close proximity to diffuse ganglion cells (DG) but without making a direct contact. Instead, the rod BCs contact two types of AC, the AII and the A17. (Drawing courtesy of Dr. Helga Kolb)

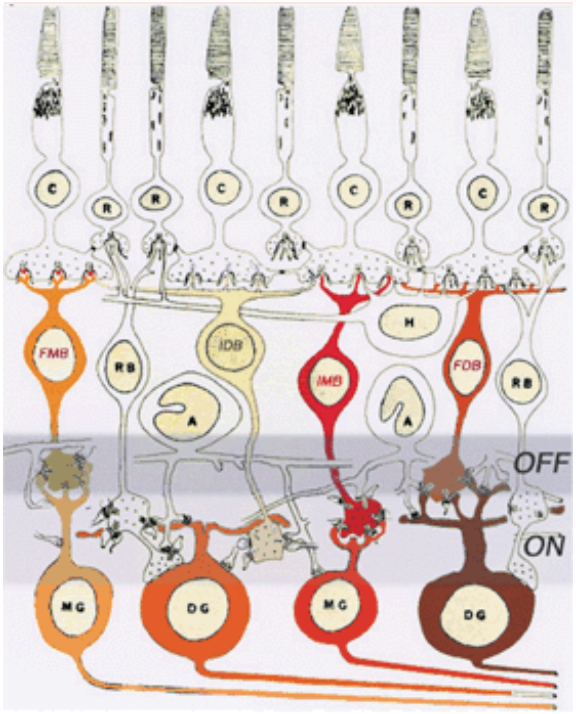

Figure 18. Diffuse and midget BC pathways of the primate retina and the ON-OFF lamination of the retina.

The axons of flat midget BCs (FMB) terminate in the distal portion of the inner plexiform layer, which is the OFF zone, whereas those of invaginating midget BCs (IMB) terminate in the proximal portion of the inner plexiform layer, the ON zone. Rod BC axons (RB) and those of invaginating diffuse bipolars end in the ON zone; those of flat diffuse bipolars (FDB) end in the OFF zone. (Drawing courtesy of Dr. Helga Kolb)

lation include the presence of Transient Receptor Potential (Canonical) or TRPC channels in photoreceptors (61). This orchestra of channels and pumps serve to monitor and regulate the basic Ca^{2+} levels necessary to maintain glutamate release.

BIPOLAR CELLS IN MAMMALIAN RETINAS

A typical mammalian retina has over ten BC classes (e.g. Fig. 2,16), one driven exclusively by rods and the others by cones (7, 62). BCs also subserve a major func-

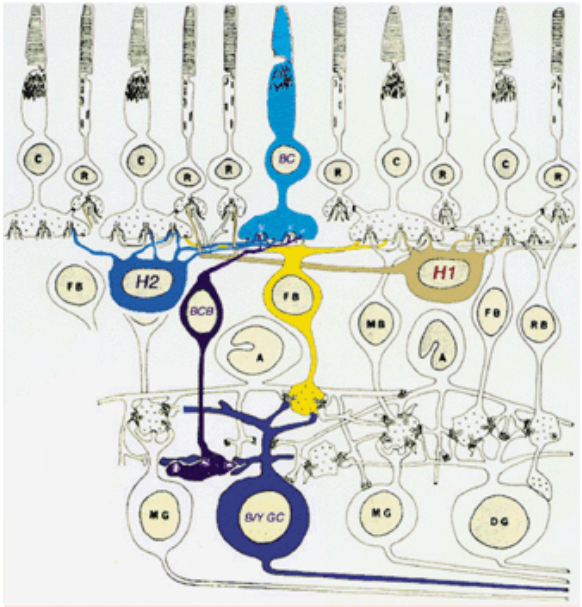

Figure 19. The blue cone BC pathway of the primate retina.

Blue cone contacting BCs (BCB) make invaginating contacts with blue cones (BC) in the outer retina. The blue cone bipolar axon terminal provides input to a blue/yellow color coded ganglion cell (B/Y GC) in the inner plexiform layer. The yellow surround is provided by diffuse cone bipolars (FB), which contact both L and M cones at basal junctions. Other cell types: C, cone; R, rod; DFIG and H2, HCs, MB; midget bipolar; RB, rod bipolar; A, AC; MG, midget ganglion cell; DG, diffuse ganglion cell. (Drawing courtesy of Dr. Helga Kolb, based on Dowling JE, Boycott BB: Organization of the primate retina: Electron microscopy. Proc R Soc Lond Biol 166:80, 1966)

tional organizing principles for the visual system: the generation of separate ON and OFF channels. ON BCs respond to light with graded voltage depolarizations and have long axons ending deep in the IPL. OFF BCs respond to light with graded voltage hyperpolarizations and have short axons ending high in the IPL. Rod BCs are ON cells (Fig. 17), comprise about 40% of all BCs and have densely branched dendritic arbors contacting 20 to 30 rods at ≈ 1 mm from the fovea and roughly twice that number in peripheral retina (30). Cone BCs cells come in several classes. Midget BCs (63) found in primate and squirrel retinas each contact a single cone in the fovea, but in peripheral retina may contact more than one cone. Midget BCs contact LWSR or LWSG cones (Fig. 2,18), but are thought not to contact SWS1B cones by some authors (64). Others argue for the presence of a midget OFF BC selective pathway (65). Most of our knowledge of B cone signaling involves a unique non-midget ON BC that selectively contacts a sparse collection of B cones (66). However, the concept of a predominantly pure ON blue pathway has received further challenges by discovery of blue-selective OFF BCs in rabbit retinas as well (67). Midget BCs typify two types of relationships between cone synaptic terminals and BC dendrites. ON midget cells make *invaginating* dendrites forming a central member of the synaptic triad at ribbon synapses. OFF midget cell dendrites end as a flat (basal) junction on the surface of the cone. Each central LWSR and LWSG innervates many copies of ON and OFF midget bipolars (Figure 11).

The dendrites of B cone-specific ON BCs (66) are long and sparse compared with those of a midget BC, as blue cones are a minority (7%-10%) of the cone population and are widely spaced. Blue cone-selective ON BCs typically contact only two or three cones. The density of these BCs is highest in central retina although at the foveola there are presumably fewer as the blue cones density drops in the foveal pit (19). The dendrites of blue cone BCs are invaginating and the axons terminate in the proximal portion of the IPL (Fig. 19). Diffuse BCs seem to contact all cone types but statistically contact fewer B cones (68). Primates may also have OFF center diffuse BCs equivalent of ground squirrel diffuse OFF BCs that completely avoid B cones.(69). Several morphological classes of both ON and OFF diffuse BCs are also known (Fig. 18), and it the full physiological meaning is only known emerging, but clearly has to do with molecular tuning of

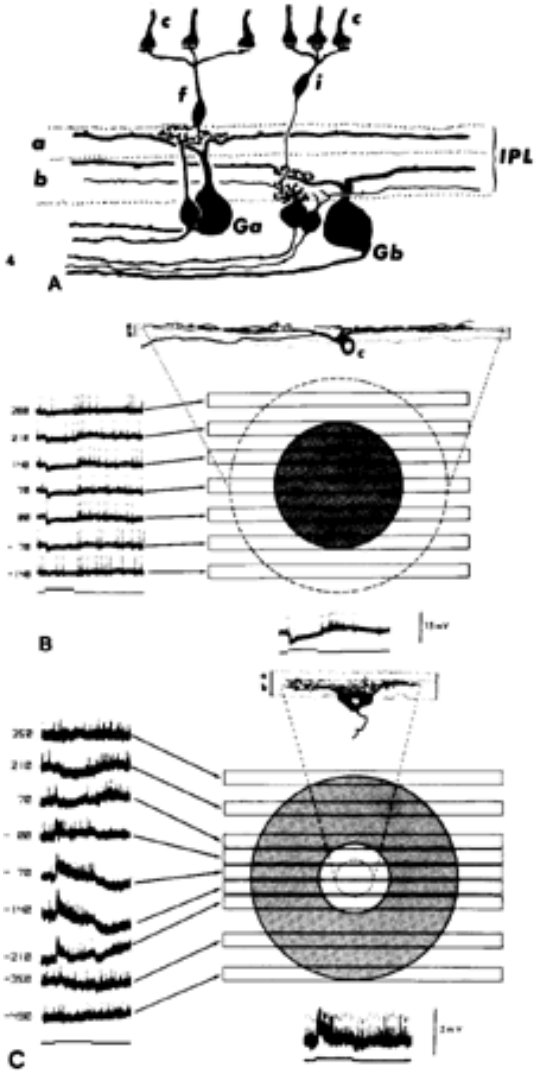

Figure 20. A. Center-surround organization of cone BCs and GCs in the cat retina.

Flat cone BCs (f) have axon terminals that end in sublamina a and contact the dendrites of Ga-type ganglion cells. Invaginating cone BCs (i) have axon terminals that ramify at a more proximal level of the IPL in sublamina b, where they contact Gb-type ganglion cells. Ga cells are off-center and Gb cells are on-center ganglion cells. c, cones. B. Receptive field properties and morphology of an intracellularly stained off-center ganglion cell. Note the dendritic arborization in sublamina a. At left are shown responses to slits of light positioned at different levels of the receptive field. They show that a hyperpolarization (inhibitory postsynaptic potential) is elicited when the slit is positioned between 210 µm and -70 µm (shaded circle). The dotted circle gives the dendritic field of the cell as 490 µm. The response to a diffuse stimulus is shown at bottom. (Stimulus width, 50 µm; duration, 542 msec; wavelength, 441 nm; intensity, 2.7 log quanta µm-2 sec-1). c, cone. C. Concentrically organized on-center ganglion cell of the rat retina. The dendritic arbor of this cell is confined to sublamina b of the IPL. The membrane depolarization (excitatory postsynaptic potential) is elicited by light stimuli falling between 0 and 210 µm (open circle). The dotted circle indicates the subtense of the cell's dendritic arbor. The shaded circle indicates the spatial extent of the inhibitory surround. (Stimulus width, 100 µm; duration, 560 msec; wavelength, 647 nm; intensity, 4.6 log quanta µm-2 sec-1) (Nelson R, Famiglietti EV Jr, Kolb H: Intracellular staining reveals different levels of stratification for on- and off-center ganglion cells in cat retina. J Neurophysiol 41:472, 1978)

BCs for sensitivity and speed. The axons of diffuse BCs end in distal and proximal portions of the IPL and are associated with specific subsets of ganglion cell.

HORIZONTAL CELLS IN MAMMALIAN RETINAS

HCs are gliaform cells that serve as the lateral inhibitory interneurons of the outer retina. Most mammalians have axonless and axon-bearing HCs, though some (mouse and rat) have only axon-bearing HCs(70-72). HC somatic dendrites selectively contact cones, while HC axon terminal (HCAT) dendrites generally contact only rods. It important not to confuse the HCAT with axonal fields of true multipolar neurons. HCs do not spike and mammalian HC axons appear to serve only as trophic support for the large cell-like HCAT (73). Primates have 2 or 3 classes (Fig. 2) of HCs (74). Class H1 contacts both LWS and SWS1 cones and comprises about 80% of all HCs. Their physiological responses are yellow-dominated (Y=R+G). Class H2 cells comprise about 20% and are enriched for blue responses, as they tend to contact more SWS1 cones than H1 cells. Class H3 HCs have been described by the Golgi method (75), but have as yet no known molecular signature that would allow them to be found by an independent method. Primate HCs contact about a dozen cones in the foveola and nearly two

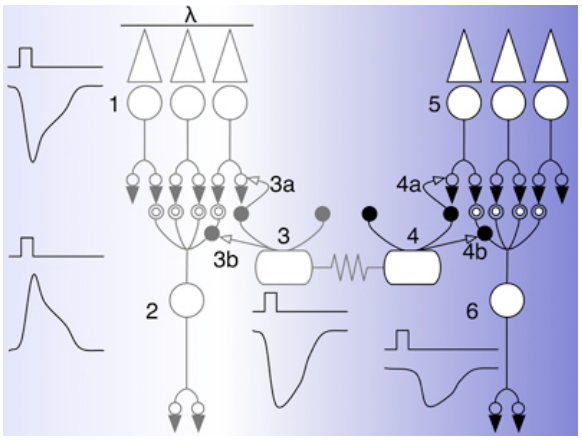

Figure 21. Paths for HC-mediated center-surround signaling.

A. At left, (1) cones are hyperpolarized by light which depolarizes (2) ON BCs hyperpolarizes (3) HCs. HCs can provide sign-inverting local feedback (3a) or sign-conserving local feedforward (3b). As HCs are coupled by gap junctions, the hyperolarization spreads to (4) neighbor HCs connected to (5) cones in the dark. The sign-inverting lateral feedback (4a) evokes a cone depolarization which leads to hyperpolarization of the connected (6) ON BC. Conversely, the sign-conserving lateral feedforward (4b) directly hyperpolarizes the ON BC.

dozen in the periphery. In the rod-free region of the central retina, H1 cells are axonless but do display HCATs in the periphery, contacting a few hundred rods in primates. Homologous HCATs in non-primate (type B HCs in cat and rabbit) contact perhaps a thousand rods. HCATs in most mammals have exclusively rod-driven responses, with no evidence of cone signals, which is further evidence of the lack of axonal signaling. HCs engage in extensive homologous (in-class) coupling. The equivalent of primate H1 cells is the rabbit type B axonal HC, which has moderate somatic coupling (48, 76). Primate H1 and H2 cells do couple across classes, and form completely separate mosaics (76, 77) The axonless type A HC of the rabbit has no homologue in primates, and is extensively coupled (48). HCs are also unusual in directly contacting arcade c3 endothelial cells mammals (12), further suggesting glial attributes.

PHOTORECEPTOR → HC AND BC SIGNALING

Photoreceptor signals to BCS and HCS are decoded by glutamate receptors of two groups: tetrameric assemblies of transmembrane ionotropic glutamate receptor (iGluR) subunits and single protein heptahelical, metabotropic glutamate receptors (mGluRs). The iGluRs are one of three distinct superfamilies of ligand-gated ion channels. The mGluRs are not channels at all, but GPCRs linked through several transduction pathways to cellular modulators. The details of these receptors in vision have been reviewed extensively (3, 7). In broad terms, iGluRs are subdivisible into (i) AMPA and kainate (KA) receptors that *directly* mediate synaptic drive by opening cation channels and (ii) NMDA receptors that act as as complex coincidence detectors, requiring simultaneous glutamate-binding, membrane depolarization and a co-receptor activation. D-serine is the likely co-receptor ligand (78). AMPA and KA receptors mediate signaling in the OPL, while AMPA and NMDA receptors function in the IPL (79, 80). AMPA or KA holoreceptors are formed by four homologous protein subunits with three membrane spanning segments each. AMPA are co-assemblies of GluR1-4 subunits and KA receptors are co-assemblies of GluR5-7 + KA1,2 subunits. Many subunits have splice and RNA-editing variants, allowing for significant complexity in receptor properties and trafficking. AMPA and KA receptors admit a variety of subunit mixtures, bestowing the holoreceptor with a range of glutamate affinities, unitary conductances, kinetics, modulation and trafficking regulation. HCs decode photoreceptor glutamate signals with AMPA receptors (81) and con-

tain GluR4 and GluR2/3 subunits (82). Some OFF BCs express AMPA receptors while most express KA receptors (83). AMPA and KA receptors provide a canonical sign-conserving synapse.

The mGluR superfamily is complex and many mGluRs are expressed in the mammalian retina (3). The mGluR6 receptor is a group C obligate-dimer and decodes photoreceptor glutamate signals in rod and cone ON BCs in a sign-inverting mode. The mGluR6 transduction pathway is poorly understood, but likely involves a Goα-type G-protein (84) whose activation via glutamate binding mediates *closure* of a non-selective cation channel with high calcium permeability. Cone hyperpolarization slows synaptic release and accelerates EAAT2 uptake (85), the rapid drop in glutamate concentration leads to inactivation of mGluR6 and depressed inhibitory signaling. BC cation channels open and the inward current depolarizes the ON BC. We do not yet know the nature of those channels. Recently, another group C family member, the mGluR7 receptor, has been found in association with some cone ON BCs (86). Its selective role remains unknown.

Differential expression of glutamate receptors by BCs creates parallel ON and OFF channels in vision. In general, ON BCs express mGluR6 receptors and OFF BCs express either AMPA or KA receptor pharmacologies. But Hanna and Calkins (87) have clearly shown that primate ON BCs also express a cohort of AMPA receptors, even though mammalian ON BCs display no robust iGluR currents (80). This suggests a complex role for receptor trafficking and turnover as a key regulator of BC functional identity. Further, Marc et al.(88) recently showed significant plasticity in rod BCs of human retina in cone-sparing forms of retinitis pigmentosa where loss of rods, but not cones, led to phenotype switching from ON to OFF in rod BCs. The fact that normal rod BCs express iGluR subunits argues that such switching is within the normal capacity of BCs. The difference between *expression* (mRNA synthesis) versus *display* (properly inserted transmembrane proteins) is *terra incognita* at present.

A great deal of our understanding of parallel information processing channels is based on the differential pharmacologies of iGluR/mGluR pathways. This large literature is reviewed in Marc 2004 (3). Thus mGluR6 receptors drive the canonical ON (sign-inverting) and iGluR receptors drive the canonical OFF (sign-conserving) pathways. But even within the iGluR group there is finer granularity. The majority of OFF BCs in ground squirrel express KA receptors, which are highly glutamate-sensitive. This raises the issue that AMPA, KA and mGluR6 receptors differ in their glutamate affinity and response kinetics and this is reflected in the patterning neuronal dendrites around ribbon synapses (Fig. 8). Vesicle fusion occurs on either side of the synaptic ribbon and glutamate diffuses along a gauntlet of pre-synaptic glutamate transporters. Thus the rapidly desensitizing AMPA receptors of HCs are the closest to the photoreceptor release site and actually respond to light with a smooth progression of channel closures from a highly desensitized state. Next, the invaginating dendrites of ON BCs strategically position mGluR6 receptors a little further away, and the semi-invaginating dendrites of OFF BCs expressing AMPA receptors appear a bit further afield. Finally, ringing this complex of processes are the KA receptor expressing OFF BCs forming classical flat contacts. When a vesicle

fuses, most of the glutamate is recaptured by glutamate transporters on photoreceptors or MCs, while receptors distant from the site of release experience levels some 10-100x lower.

INFORMATION PROCESSING IN THE MAMMALIAN OUTER PLEXIFORM LAYER

Nocturnal rod vision emphasizes sensitivity. diurnal cone vision emphasizes acuity, contrast and speed. Unlike non-mammalians, which display BCs with mixed rod-cone inputs, mammalian rod and cones in mammals target distinct rod and cone BCs. Rod BCs are a single class of mGluR6-driven ON BCs and at least 10-12 classes cone BCs exist: roughly half as ON BCs expressing predominantly mGluR6 receptors and the other half as OFF BCs expressing either KA or AMPA receptors. The switch from scotopic to photopic processing in mammals is not completely understood except insofar as rods saturate and cones become responsive.

The essential role of a cone BC is to develop a neural contrast signal. Its direct center cone inputs combines with signals derived from an indirect or surround field of photoreceptors. Cone BCs have a small dendritic spread, which delimits the center, and the surround signal derives from the HC sheet into which each BC is inserted. This contrast signal has been recorded from the retinas of non-mammalians (fishes, amphibians, reptiles) and its also present in mammals (89). Further, the HC contrast signal is readily readily detected in the responses of retinal mammalian GCs (90, 91). Figures 20 and 21 outline the conceptual flow of signals that generate contrasting center and surround pathways.

The centers of ON and OFF pathways are created by BC functional display of mGluR6 and AMPA/KA receptors respectively which decode photoreceptor synaptic glutamate release. However the signaling mechanism of HC feedback remains a mystery. First, it is unclear whether signaling is mediated primarily through feedback to cones (pathway 1 → 3 → 4a →5 → 6 ; Fig. 21), feedforward to BCs (pathway 1 → 3 → 4b → 6 ; Fig. 21), or both; or even whether the pattern is different for different classes of BC → GC networks. Understanding synaptic chains is aided by tracking response polarities at synapses or gap junctions. Classical excitatory processes conserve the sign of a signal transfer while nominal inhibitory processes invert the sign, equivalent to multiplying by a constant -k. Thus an entire chain of synapses can be characterized as net sign-conserving or sign-inverting based on whether the number of inversions is even or odd. Odd total inversions denote a net sign-inverting chain. Another way to use this idea is to observe the the outcome of a chain (e.g. center or surround) and determine the synaptic polarities required to achieve it. Here is how we might generate centers and surrounds in ON BCs in Fig. 21.

Depolarizing Center:
cone 1 $>_m$ ON BC 2 (mGluR6)

Local Hyperpolarizing feedback:
cone 1 > HC 3 $>_i$ cone 1 $>_m$ ON BC 2

Local Hyperpolarizing feedforward:
cone 1> HC 3 > ON BC 2
Far Hyperpolarizing Surround feedback:
cone 1> HC 3 $>_i$ cone 5 $>_m$ ON BC 6

Far Hyperpolarizing Surround feedforward:
cone 1 > HC 3 > ON BC 6

Similarly for centers and surrounds in OFF BCs in Fig. 21.

Depolarizing Center:

cone 1 > OFF BC 2 (AMPA or KA receptors)

Local Hyperpolarizing feedback:
cone 1HC 3 >$_i$ cone 1 > OFF BC 2

Local Hyperpolarizing feedforward:
cone 1 > HC 3 >$_i$ OFF BC 2

Far Hyperpolarizing Surround feedback:
cone 1 > HC 3 >$_i$ cone 5 > OFF BC 6

Far Hyperpolarizing Surround feedforward:
cone 1 > HC 3 >$_i$ ON BC 6

These chains highlight a persistent problem about surround signals in the outer plexiform layer: we don't know how HCs signal to other neurons. While there is abundant evidence that some (but definitely not all) HCs in non-mammalians may use GABA as a transmitter (92), the evidence in mammals is weak and circumstantial at best (3, 7). There are three distinct hypotheses for how mammalian HCs generate antagonistic surrounds in cone BC pathways: (1) synaptic release of GABA or an unknown transmitter; (2) field currents generated by hemichannels that modulate cone synaptic release; (3) pH regulation cone synaptic release. It is possible that multiple mechanisms operate. Each hypothesis has serious defects.

The *vesicular release hypothesis* is driven by the variable presence of GABA in HCs. GABA is expressed in primate HCs within ≈ 2 mm of the fovea, but not in peripheral retina (93), In other mammals, HC GABA expression is similarly diverse and regional/cell class variations remain unexplained. GABA expression it is common in carnivore HCs . Lagomorphs possess GABA+ HCs in the central retina in class A HCs but not in the more abundant class B HCs. Rodents do not express GABA in HCs except early in development or possibly in strain variations. The idea that HCs use synaptic release of GABA or for feedback at cones (94) is compromised by the inability of GABA antagonists to alter the large surrounds of GCs (90, 91). So far, the idea that another transmitter might be involved (glutamate, β-alanine, etc) lacks molecular support. Finally, the lack of presynaptic specializations in HC dendrites at cone pedicles has posed a barrier to conventional models. Even so, there are vesicles in HC dendrites and even vesicle clusters in rod HCATs. However, neurons use non-synaptic vesicle fusion to deliver receptors to postsynaptic sites, so the presence of a complete constitutive vesicle fusion molecular cascade is not *a priori* evidence of regulated neurotransmitter release. On the other hand, classic presynaptic specializations are often evident at HC → BC contact sites proximal to photoreceptor synapses in the outer plexiform layer and GABA$_C$ receptors have been localized to mammalian BC somas and the OPL (95). The latter observation is complicated by the evidence that GABAergic interplexiform cells make conventional synapses on BCs in the outer plexiform layer (3). Regardless of whether the vesicular model is correct, all models of potential signal flow illustrate a fundamental problem first articulated by Naka: HC → ON BC signaling must be sign-conserving and HC → OFF BC signaling must be sign-inverting. Currently, the only viable model that supports this phenomenon is based on the idea that feedforward is GABAergic, decoded by GABA$_C$-like receptors that gate chloride conductances [g_{Cl}]. The direction of current flow is thus determined by the chloride reversal potential, which has long been suspected to be dynamic and influenced by chloride transport. There is evidence that the dendrites of ON BCs have elevated $[Cl]_i$ (96) so that an increase in g_{Cl} will lead to a net outward anion current, electrically equivalent to an inward cation current and a conductance increase in response to a presumed tonic HC

transmitter dark release . When HCs hyperpolarize in response to light, the distal dendrites of ON BCs will show a sign-conserving hyperpolarization. Since OFF BCs lack a dendritic chloride import process, they will exhibit a sign-inverting depolarization, in theory. On balance, the vesicular hypothesis has enough provocative attributes to remain plausible, but key evidence is missing. Finally, while some non-mammalians show a non-vesicular reverse transport of GABA at cone pedicles which may be decoded by GABAC-like receptors, mammalian HCs lack GABA transporters.

The *hemichannel hypothesis* is based on the idea that the architecture of the cone synapse is highly sensitive to field potentials generated by the presence of open connexin-based hemichannels on HC dendritic tips close to the voltage-gated calcium channels (VGCCs) of the cone ribbon synapse (97) . The theory is that, when HCs hyperpolarize, the open connexins form a path highly permeant to cations and this locally depletes the extracellular region around the ribbon, decreasing the electrochemical potential difference between the intrapedicle and extracellular space, activating VGCCs and generating a net release of glutamate, which would depolarize the HC after a slight delay. Evidence for this hypothesis has been growing slowly but consistently including the expression of Cx55.5 at zebrafish HC dendritic tips, and the apparent blockade of a feedback transient in cones by agents that block gap junctions (97). A key limitation of the hemichannel hypothesis is that it cannot account (yet) for feedforward properties.

The *proton hypothesis* derives its strength from several studies that demonstrate the ability of strong physiological buffers such as Good's buffers (98) to block HC → cone feedback signals and, more specifically, block the large, uniform surrounds of ganglion cells (99). The concept underlying the proton model again focuses on presynaptic calcium channels, where acidification of the extracellular synaptic space shifts the voltage dependence of the VGCCs to positive values and alkalinization shifts it to negative values. Thus, hyperpolarization of HCs is thought to permit alkalinization of the extracelluar space near the VGCCs and induce a higher rate of calcium entry, facilitating synaptic glutamate release. Very strong support for this model has emerged from the successful use of HEPES buffer to eliminate strong opponent surrounds in retinal ganglion cells, especially the Y- surrounds of B+ cells. Furthermore, Field et al. (91) showed that the Y- surround was also blocked by AP4, arguing that the surround path was indeed driven by feedback: R+G cones > HCs $>_i$ B cones $>_m$ B cone BCs > B GCs.

On balance, the proton hypothesis has the strongest support at present, although the molecular mechanism is quite uncertain. Further, Baylor, Fuortes and O'Bryan (100), Fuortes, Schwartz and Simon (101) and others have shown that HC feedback to cones in turtle directly evokes a voltage change, something that neither the connexin nor proton hypotheses explicitly predicts unless the induced VDCC current is very large. And the presence of GABA in some mammalian HCs remains a provocative mystery, as is the presence of small vesicles in the HC dendrites. Nevertheless, these recent data strongly support the idea, first obtained in fishes using two-electrode experiments (102) that large GC surrounds

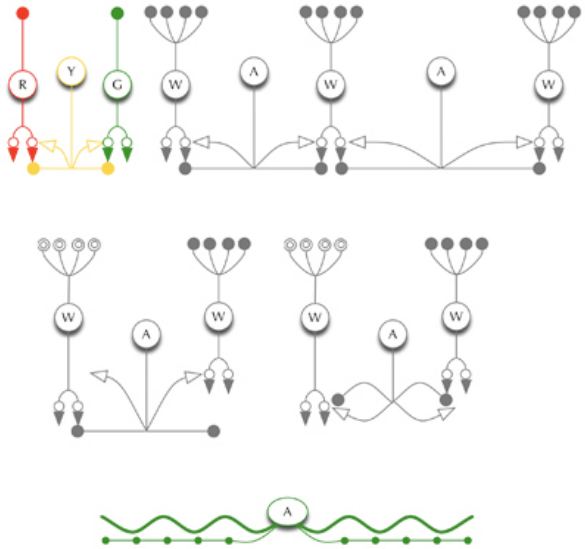

Figure 22. Canonical AC classes.

ACs make conventional synapses on BCs and GCs (not shown). Top: So-called medium-to-wide-field ACs (which includes midget ACs, paradoxically) process signals within a layer of the inner plexiform layer, typically involving one class of BC. Middle: Narrow-field ACs tend to process signals across layers. Bottom. Axonal cells collect inputs on their dendrites and generate action potentials that drive synaptic terminals on fine, long axons.

are predominantly derived from HC signals.

DIVERSITY OF AMACRINE AND AXONAL CELLS

ACs are members of Superclass 2, multipolar neurons, and their neurites comprise the bulk of the IPL. Most ACs are GABAergic and the remainder glycinergic (3, 103). Some are mixed function cells, such as the dual GABAergic / cholinergic starburst ACs present in all vertebrate retinas. ACs lack classical axons and axon terminal arbors. Rather, dendrites radiate from ACs in diverse patterns and display both presynaptic and postsynaptic specializations, similar to olfactory mitral cells. These mixed-function processes are not homogeneous, however, and different classes of ACs display complex patterning , with some dendrite regions predominantly postsynaptic and others presynaptic. Partly correlating with the size of the dendritic arbor or length of dendrites, ACs display varied degrees of spiking behavior, differing from Superclass 1 photoreceptors BCs, and HCs.

On anatomical and molecular criteria, a typical mammalian retina harbors at least 30 classes of ACs (104) although the final number may be much higher (105) There are two major dichotomies among ACs based on lamination and spread (Fig. 22): lateral vs vertical and wide-field vs narrow field (7). Lateral, wide-field ACs have dendrites that tend to collect and distribute signals *within* a layer of IPL and are predominantly γ ACs. The best known forms of this cell class include the γ rod "A17" AC of sublamina c (see Fig. 17) and the γ-ACh starburst ACs of both the ON and OFF cone driven pathways. Vertical, narrow-field ACs have dendrites that tend to collect signals in one layer and distribute them to another, thus signaling *across* layers, and are predominantly glycinergic. The best known forms of this class include the gly AII rod AC that collects from rod BCs in sublamina c (Fig. 17), forms gap junctions with ON cone BCs in sublamina b and sign-inverting glycinergic synapses onto OFF cone BCs in sublamina c. Medium-field ACs tend to be diffuse and mix the attributes of lamination and spread, but most of these are likely to be γ ACs. ACs have provided an interesting test bed for the concept that molecular profiling can discriminate cell types. In a comprehensive immunocytochemical analysis of the mouse retina (106) using antibodies against calcium-binding proteins, neurotransmitters, and other markers discovered mixed patterns of detection, suggesting that finding a single univariate marker for each class is unlikely. Conversely, multivariate profiling of the AC cohort is more

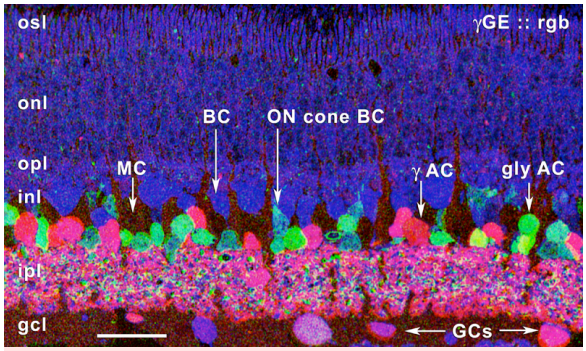

Figure 23. Neurotransmitter visualization in the mammalian retina.

GABA, glycine and glutamate (γGE) are mapped as a red, green, and blue (rgb) image. All photoreceptors show rich blue glutamate signals, as do BCs. Glycinergic and GABAergic ACs form separate populations. MCs lack any significant signal. GCs show mixtures of glutamate (their neurotransmitter) and GABA due to heterologous coupling with GABAergic ACs. Similarly, ON cone BCs show green glycine signals due to heterologous coupling between glycinergic ACs. Marc, unpublished data.

likely to generate a strong parsing of ACs into major superclasses and even ultimate classes (93).

ACs can also be classified electrophysiologically (107-110). Further, ACs in a variety of species show very center-surround receptive field patterns (111) reminiscent of those expected (but rarely observed) in mammalian BCs . This was articulated most elegantly by Sakai and Naka in catfish retina where specific ON and OFF sustained (nonspiking) of ACs driven directly by BCs exhibited a strong central light response surrounded by a narrow ring of opposite polarity, and further surrounded by a broader weaker ring of center polarity (112). This is consistent with the potential organization of γ ACs as lateral sheets of nested feedback networks (113). Similar patterns of organization have been reported for mammalian ACs, implying a fundamental network motif has been preserved across vertebrate taxa. Collectively, ACs manifest a greater repertoire of light-evoked responses than HCs. Further, very fine-scale events such as oscillations in light responses have also been documented as likely arising from local γ AC feedback(114). Indeed, this suggests that ACs are instrumental in forming fine-scale (fast, local) trigger features for retinal GCs rather than simple contrast control offered by HCs (115). For example, HCs have relatively slow response kinetics and so are unsuited for retinal circuits concerned with the neural coding of motion and direction of movement; this is accomplished by γ ACs as will be discussed below.

Another recently re-discovered feature retinal function is the presence of sparsely distributed axonal cells (AxCs) that have long, smooth axon-like processes that may extend up to a few millimeters (116, 117), all confined to the retina, resembling intraretinal ganglion cells. The neurochemistry of this group of neurons is poorly understood, but it appears that at least one of the AxC cohort, TH1 DA cells, may actually be wide-field excitatory neurons.

NEUROCHEMISTRY

The neurochemistry of the mammalian retina has been reviewed in detail (3, 7). While a great number of transmitter candidates have been found in the retina (Fig. 23), the major five that perform the vast majority of critical signaling are glutamate, GABA, glycine, acetylcholine and dopamine.

Glutamate: As noted earlier, all neurons in the canonical vertical chain from cones to cortex are glutamatergic, whereas almost all other retinal neurons use either the fast inhibitory neurotransmitters GABA or glycine. The retina represents a quintessential heterocellular metabolic circuit that partitions glutamate metabolism into dif-

(A) [E]VES → synaptic release → [E]O → SLC12345 MC import → [E]MC

(B) [E]MC → glial GS → [Q]MC → SLC76543 MC export → [Q]O

(C) [Q]O → SLC544545 neuron import → [Q]N → neural PAG → [E]N → VGLUT → [E]VES

… where the subscripts denote the vesicular (VES), extracellular (O), Müller cell (MC), and neural (N) compartments, SLCs are transporters, GS is glutamine synthetase and PAG is phosphate activated glutaminase.

ferent compartments. In mammals, a distinctive neurovascular pathway provides a complete carbon skeleton processing path whereby glucose and other precursors are collected from the endothelia via MCs, partly transformed and then delivered to neurons. The most elegant path is the the glutamine (Q) - glutamate (E) cycle. Neurons are unable to make glutamine, which requires free ammonia, yet they require glutamine for glutamate synthesis. This is achieved by a single transcellular exchange:

(A) [γ]VES → synaptic release → [γ]O → SLC12345 MC import → [γ]MC

(B) [γ]MC → MC GABA-T → [αKGA]MC → MC AAT → [E]MC

GABA (γ): In mammals (but not in ectotherms), this cycle is further exploited by the presence of GABA transporters on MCs which capture GABA carbon skeletons and drive further E production, thus blending γE and QE cycles.

Glycine: The metabolism of glycine is poorly understood and controversy still exists over the idea that gly ACs acquire their glycine via transport from the extracellular space (3, 118). It is also probable that gly ACs can synthesize glycine *de novo* via the alanine-glyoxylate transferase pathway, though this has not yet been proven.

Other transmitters: The neurochemistries of ACh ACs and DA AxCs are apparently conventional and have been summarized recently (3). More complex and certainly much less understood are the regulation of peptidergic and nitrergic systems. The former include a set of opiod and non-opioid peptides produced by conventional protein synthesis and post-tranlational processing to yield high potency co-transmitters of wide-field γ ACs packaged as dense-core vesicles and apparently under different vesicle fusion regulation than the fast transmitters. These include substance P, somatostatin, vasointestinal peptide, and neuropeptide Y. Their physiologies and anatomies have been reviewed recently(119), but we still have a minimal view of their roles in vision.

SIGNAL PROCESSING IN THE INNER RETINA

The IPL marks the transition in signal processing from simple, low spatial frequency surround signals generated by HCs, to fast, high spatial frequency, and often complex

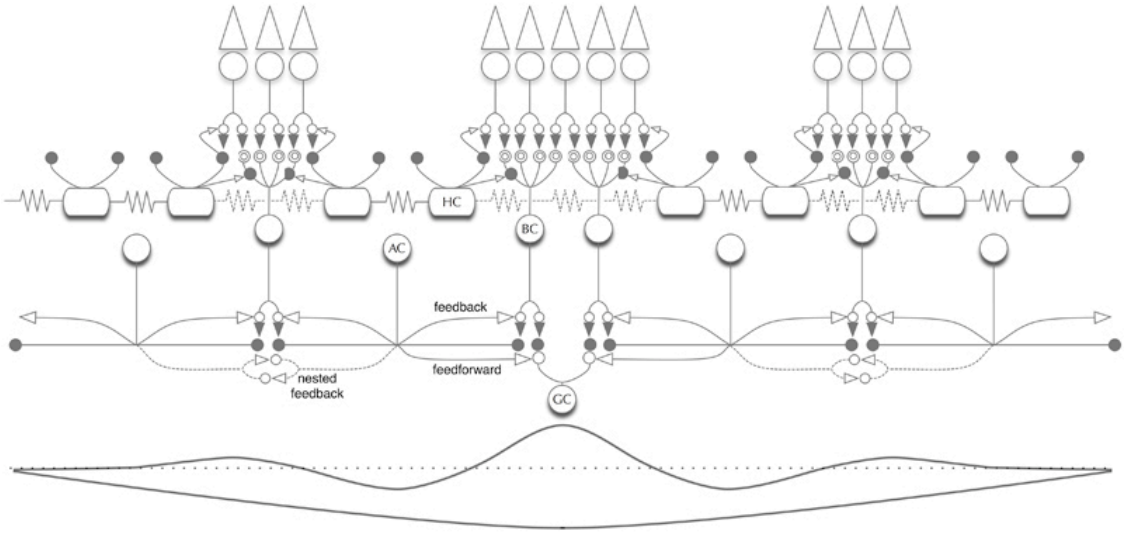

Figure 24. Canonical achromatic ON pathways.

A summary of all the pathways collected by one GC in forming the receptive field. The HC networks follow the patterns of Fig. 21. ACs make three kinds of connections: (1) BC → AC → BC feedback submotifs; (2) BC → AC → GC feedforward submotifs; (3) BC → AC → AC → BC or GC nested feedback submotifs. The bottom profiles show the combined BC + AC and HC effects. ACs are small field and, as shown by Naka, themselves have center-surround organization. When summed this creates a narrow and fast near surround and successively larger and weaker wavelets of disinhibition and inhibition. Conversely, HC surrounds are large, slow and uniform due to coupling. © Robert E. Marc, 2008.

surround signaling. This is engaged by driving ACs and GCs with high-gain BC synaptic ribbons and modulating the performances of BCs, ACs themselves and GCs with an array of feedback, nested feedback, feedforward and nested feedforward networks mediated by conventional (non-ribbon) synapses (113, 120). The basic signal flow in retinal circuits is summarized in Figure 24.

BC terminals, like those of photoreceptors, possess synaptic ribbons but there is no prominent invagination of the BC since its entire surface is used for presynaptic and postsynaptic connections. Most often two processes are postsynaptic to each BC ribbon, and typically they are AC-AC pairs, less often AC-GC pairs. In central retina of primates, the midget system of invaginating ON and flat OFF BCs respectively target separate ON and OFF midget GCs in sublamina b and sublamina a respectively.

In the case of midget BCs, all ribbon synapses are made with a single GC. As each midget BC collects signals from a solitary cone, this forms a single cone → single BC → single GC channel. However, each cone contacts many midget BCs, and its signal is copied in a cluster of parallel channels (63, 121). Whether this degeneracy has functional importance in retina is not yet known, but it could be part of a signal coincidence mechanism for sorting chromatic signals in the brain.

The number of synaptic outputs of a single BC terminal ranges from a high of 55 to 80 in midget cone BCs (63, 122) down to about 23 ribbon synapses in rod BCs (123). In addition, there is a correspondingly large synaptic input from ACs. Often, BC → γ AC synapses are arranged in a reciprocal manner, with a corresponding γ AC → BC synapse from involving the same pair of processes (Fig. 25). In classical am-

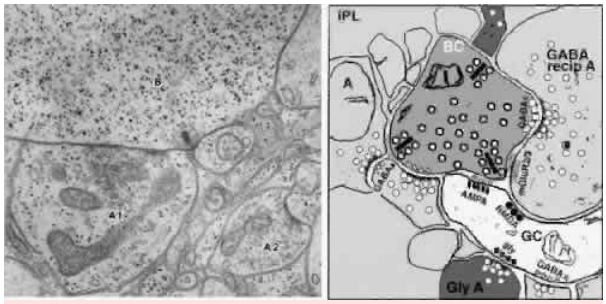

Figure 25. The anatomical substrate of feedback.

The left side is an electron micrograph of a bipolar ribbon synapse in the inner plexiform layer of the carp retina. An amacrine process (A1) receiving input from the BC (B) makes a reciprocal synapse back onto the BC terminal. A second amacrine process (A2) synapses onto an unidentified process (× 25,000; data of P. Witkovsky and J. Dowling). The right side is a schematic of the synaptic arrangement at left with the addition of the different neurotransmitter receptor types participating in information exchange. (Courtesy of Dr. Helga Kolb)

plifier theory, the purpose of negative feedback is to precisely control the gain, reduce noise and enhance the bandwidth of an amplifier. In retina, it is believed that γ ACs sample the BC output and provide a scaled inhibitory feedback that truncates the BC output (124). Most of these are γ ACs and BCs predominantly GABAc receptors on their terminals, and GABA gates a small, high-sensitivity, sustained, largely non-desensitizing chloride current that opposes the BC depolarization (125-129). In addition, the feedforward signal to retinal GCs can enhance this inhibitory effect (124) .

ACs have diverse physiologies, some with sustained responses, some with transient, and many with spiking. How they correspond with and shape the properties of specific classes of retina GCs has not been established. This is due to several major technical problems. First, the functional correlates of anatomic diversity of BCs, ACs and GCs are incompletely understood. Second, the potential topologies of retinal circuits can be immense. A simple five element network of two different classes of BCs, two classes of GCs and a single cross-class AC can be connected in 90 unique ways and 40 of them are biologically realistic. Third, the correct formal topology is not always obvious and rarely predicts the biological topology. In general, physiological measures have been insufficiently precise to provide unique network solutions to GC properties. The most dramatic example of this is the mammalian rod pathway (130-132), which involves an arcane, bifurcating path for transmitting rod signals to GCs (Fig. 26). Despite over a half century of physiology, no single experiment correctly predicts this network's motifs, discovered by serial section electron microscope reconstruction (132, 133). In fact, most physiological and genetic experiments have been designed to test, rather than explore these motifs. Directly tracing networks remains the most powerful pathway discovery method. A further complication is that direct AC → AC synapses are among the most common in the retina (113, 120) and no model retinal circuit explicitly uses them for any known trigger feature. Previous studies in non-mammalians suggest that such synapses are part of a widespread nested feedback system that increase the bandwidth of the BC - AC - GC network without generating a large low frequency roll-off characteristic of simple feedback (113). This has not been proven physiologically however, since nested inhibitions cannot be selectively dissected (128).

THE FUNDAMENTAL ROD & CONE PATHWAYS PATHWAYS OF MAMMALS

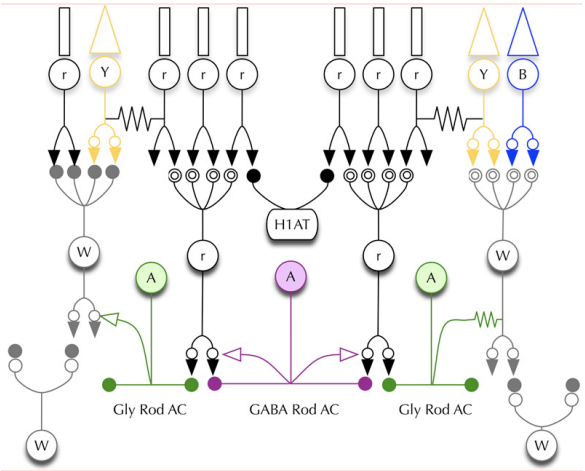

Figure 26. The three primary rod pathways.

(1) The high-gain pathway is driven by the rod BC which feeds the glycinergic (gly) rod AC, and which in turn is coupled to ON cone BCs and synaptically drives OFF cone BCs. (2) Rods can directly drive some OFF cone BCs. (3) Rod-cone coupling leaks scotopic signals into LSW cone pathways. GABA ACs provide BC feedback networks. H1ATs collect rod signals but their outputs are unclear. © Robert E. Marc, 2008.

The synaptic chains that drive GCs in all retinas are stereotyped into ON and OFF pathways. In fact, the first synapse in vision sets the polarity of a parallel channel that travels all the way to cortex: cone >m ON BC > ON GC > ON LGN > ON cortex . In non-mammalians, rod and cone pathways use this direct chain (primarily targeting tectal rather than telencephalic regions) via mixed rod-cone BCs that collect from both photoreceptor classes and directly target GCs. In mammals, a unique high-sensitivity scotopic system has evolved that uses cone BCs at the output devices, with rod BCs serving as an interneuron (134). Mammalian rod BCs appear homologous to non-mammalian mixed rod-cone BCs, but have lost both (i) cone inputs and (ii) the ability to target GC dendrites. How this evolved is uncertain. Nevertheless, five distinct rod networks from three primary pathways (Fig. 26) have been found in mammals here grouped by amplification.

3-stage amplification
(1) rods $>_m$ ON rod BCs > gly AII ACs :: ON cone BCs > ON GCs

(2) rods $>_m$ ON rod BCs > gly AII ACs $>_i$ OFF cone BCs > OFF GCs

2-stage amplification
(3) rods :: cones $>_m$ ON cone BCs > ON GCs

(4) rods :: cones > OFF cone BCs > OFF GCs

(5) rods > OFF cone BCs > OFF GCs (sparse and species variable)

(6) rods $>_m$ ON cone BCs > ON GCs (sparse)

Thus, rod vision appears fractionated into ranges served by different circuits: (i) the gly AII AC circuit with two arms of three-stage amplification for dim starlight vision and ((ii) the rod :: cone → cone BC → GC two-stage amplification path for moonlight vision. Note that bright moonlight can directly activate cone vision, and like crepuscular transitions, moonlight can be a classical mesopic domain bridging purely achromatic scotopic and chromatic photopic worlds. Recently, in addition direct rod > cone BC contacts have been documented in some mammals (86, 135-137). Whether these additional pathways are epiphenomenonal or essential is unclear as the strength of their expression varies across mammals (138).

In addition to the AII AC [termed the AII cell by Kolb and Famiglietti (132, 133)], rod BCs also drive several classes of GABAergic neurons including wide-field γ rod ACs (also known AI or A17 in cat(139) , and S1/2 or indoleamine-accumulating ACs in rabbit(140). These γ rod ACs have dendritic arbors of 1 mm in diameter and CF > 500(141), each contacting over 1,000 rod BCs with reciprocal feedback synapses, with S2 cells providing twice the number of feedback synapses as S1 (142).

As rod BCs show no strong surrounds (and dark-adapted GCs have weak surround fields), it is likely that these pathways influence the signal-to-noise ratio and the temporal transfer functions of BCs in classical operational amplifier modes.

The glycinergic AII rod AC is a pivotal neuron in the evolution of mammalian scotopic vision, for it enables the rod pathway to amplify its signal one time more through cone BC > cone GC AMPA/NMDA mediated synapses. The evolutionary antecedent of this cell is unknown but is likely to be a small-field glycinergic neuron with classic vertical arborization. The glycinergic rod AC is actually tristratified (130, 132, 133), (i) receiving rod BC inputs on its fine arboreal dendrites deep in sublamina c, (ii) forming heterocellular gap junctions via heterotypic Cx36/Cx45 gap junctions with the axons of ON cone BCs in mid-IPL, and (iii) providing output synapses predominantly onto OFF cone BCs in sublamina a. AII ACs also receive OFF cone BC inputs and feedforward to GCs, though the latter inputs are sparser. This implies that it also has a role in temporal processing of photopic inputs in the OFF pathway. The net, high-sensitivity scotopic response of mammals is thus distributed by the glycinergic rod ACs. Glycinergic ACs are driven largely by AMPA receptors with very little NMDA receptor involvement (79, 80) (but also see Zhou and Dacheux (143) and generate strong transient depolarizations to light inputs. The rod $>_m$ rod BC > AII AC chain has two stages of high-gain glutamatergic transmission, resulting in an extremely sensitive photoresponse. Further AII ACs are themselves pooled by AII AC:: AII AC coupling. While this does not amplify the signal further, it may provide some noise reduction. The AII AC distributes its depolarization by direct AC::ON cone BC coupling and by gly rod AC $>_i$ OFF cone BC synapses: both very low gain or even fractional gain steps. The final step comes via cone BC > cone GC signaling through high-gain AMPA/NMDA receptors. This network is modulated by at least four distinct mechanisms. First, rod BCs possess negative feedback through γ rod ACs and this is manifest in the presence of a fast, narrow surround in gly rod ACs (111). Second, dopamine agonists (mimicking light adaptation) appear to uncouple AII AC :: AII AC networks (49). Third, nitric oxide donors such as sodium nitroprusside that lead to activation of soluble guanylate cyclase and rapid elevation of [cGMP] $>_i$ lead to closure of AII AC :: ON cone BC gap junctions (49). Finally, each cone BC output channel has both γ feedback and feedforward. Thus the seemingly smooth and slow percept of the starlight scotopic world involve complex synaptic transitions. However, as one approaches lunar brightnesses, rod vision slowly gives way to cone vision and high amplification is no longer needed. In fact, rod BCs saturate (42). It appears that a second scotopic set of two-stage paths take over based on rod :: cone coupling. This pathway only has the gain of the cone → BC → GC chain and doesn't even have the potency of the rod $>_m$ rod BC synapse. Though less sensitive, it is nevertheless operative at intensities slightly below cone threshold. Like the three-stage ON pathway, it depends critically on Cx36-containing connexons. In Cx36 knockout mice the only remnant pathway is the OFF GC path (144).

FUNCTIONAL CLASSES OF RETINAL GANGLION CELLS

At present we believe that there are some 15-20 classes of retinal GCs (145-147), each tuned to a specific pattern of cone BC drive and AC modulation. GCs are the

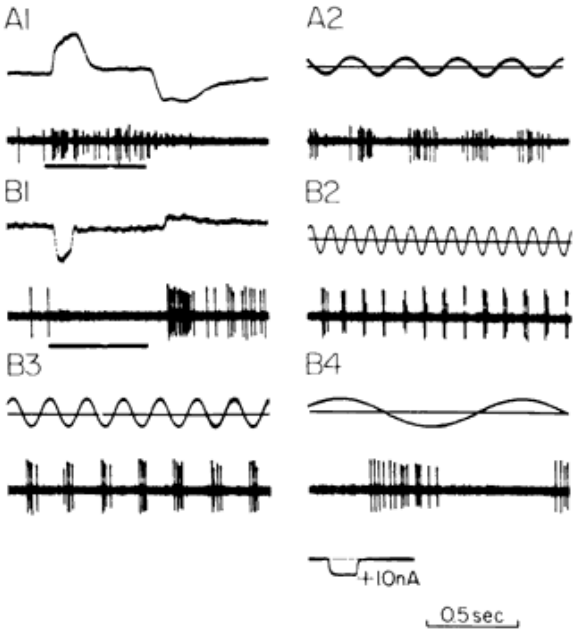

Figure 27. Activation of ganglion cells through light or injection of current into BCs.

A1. On-center BC response (upper trace) and on-center ganglion cell response (lower trace) to a light stimulus. A2. Sinusoidal current passed through the BC membrane (upper trace) evokes ganglion cell spikes (lower trace) during the depolarizing phase. B1 through B4. Comparable sets of records for off-center BC and ganglion cell responses. (Naka K-I: Functional organization of catfish retina. J Neurophysiol 40:26, 1977)

final output neurons of the retina and targets over a half a dozen CNS centers: GC > lateral geniculate nucleus LGN > CX); GC > superior colliculus SC > CX; GC > suprachiasmatic nucleus SCN > multiple targets), GC > preolivary nucleus PON > Edinger-Westfall nucleus EWN for pupillary control; and other projections (145). Many GCs classes have branching axons and target dual subcortical nuclei, such as LGN and SC.

The existence of a variety of GC morphologies has been known for a century, but the corresponding functional categories have emerged more recently. Hartline's pioneering work (148) established the ON, OFF, and ON-OFF discharge patterns exhibited by single GC cell and that many GCs of the cat had mutually antagonistic, center-surround receptive fields. He found about equal numbers of ON-center and OFF-center GCs. Critically, Kuffler (149) showed that an individual GC cell can fire bursts of action potentials after and during light onset (ON) and/or after light offset (OFF). The decisive factors include the spatial distribution of the light over the receptive field (RF) and the relative intensities of central versus peripheral light.

Subsequent work integrated these findings into the division of the IPL into ON and OFF zones (150). As illustrated in Figure 20, the dendrites of ON-center GCs arborize in sublamina b, and those of OFF-center GCs sublamina a. Naka (151) further showed, in catfish, that current injection into functionally characterized BCs activated GCs matched in class: ON BCs drove ON GCs; and OFF BCs drove OFF ganglion cells (Fig. 27). This correlation has proven true for all vertebrates.

However, GCs possess complex response tunings to stimulus parameters. The job of a GC is not simply to signal light onset and offset: even a photoreceptor can do that. For example, Enroth-Cugell and Robson (152) discovered that cat retinal GCs could be split into two functional types from a spatial summation perspective: “linear” X cells and “nonlinear” Y cells. X cells linearly combine depolarizations and hyperpolarizations over the entire receptive field, no matter how finely patterned, and give sustained discharges and often have small RFs: X cells signal structure. In contrast, Y cells are exquisitely sensitive to patterned light (specifically light-dark borders), fire transiently and have very large RFs: Y cells signal change. Later, Stone and Hoffman(153) added a third functional

category, W cells, which have a slow conduction velocity, sluggish discharge onset, and receptive fields that often lack a center-surround organization(154). Boycott and Wässle(155) subsequently matched cat GC morphological classes with large, medium and small somas (α, β, and γ cells, respectively) to broad functional groups: α ≡ Y, β ≡ X, and γ ≡ W type GCs.

In time, it became clear that the "sluggish" W category contained both sustained and transient varieties of the ON and OFF cells, while the X and Y group represented "brisk" GCs, including some dual ON-OFF cells, totaling over 8 cell classes.

Further functional types were identified in the rabbit retina including two varieties of directionally selective (DS) GCs, local edge detector (LED) GCs, orientation sensitive GCs, color opponent blue-ON/green-off (B+/G-) cells, and occasional units that yield persistent slow ON spiking to sustained lights (145, 156). We now believe the latter are the recently discovered melanopsin-expressing intrinsically photosensitive GCs of mammals (157). Thus there are no less than 15 physiological classes, closely matching the conclusions of cell injection and molecular phenotyping assessments, but likely falling short of true morphological diversity. On balance, it is likely that a few more functional types remain to be found. The primate retina is rendered more complex by the existence of midget color-opponent GCs driven by ON or OFF midget cone BCs which connect to either R or G cones, creating a further four classes.

Most mammalian retinas display a blue ON (B+) GC driven directly by blue ON BCs (158, 159). We will discuss this important cell class in more detail below, but one matter of debate has been whether blue OFF (B-) GCs exist. There is certainly evidence for this pathway at the level of the LGN and the physiology suggests that putative B- GCs are of the sluggish variety with large RFs projecting to the koniocellular layers of the LGN and to cortex (159, 160). In this regard, there is evidence that some midget OFF BCs contact B cones (65) and a diffuse BC terminating in sublamina a selective for B cones has been identified in the rabbit retina(67). After tallying every possible functional type of GC, it may not far-fetched to propose the existence of no less than 20 GC classes in the primate retina.

Finally, a major discovery has been the identification of intrinsically photosensitive, melanopsin-expressing GCs (ipGCs) : sluggish, sustained ON center GCs that have both rod and cone inputs as well as their own photopigment-driven responses (157, 161-164). These cells express a visual pigment known as melanopsin which bears closer homology to some invertebrate opsins than cone and rod opsins. Melanopsin acquires 11-cis retinaldehyde (165) through some unknown agency (perhaps MCs) and has a peak absorption around 470 nm. Cone BC and melanopsin drive appear additive, but melanopsin-gated transduction is inefficient at normal visual intensities, and only dominates cell spiking at high brightnesses. In primates, ipGCs project to the LGN, SCN and perhaps the PON (161). Thus, signaling in this pathway is conveyed to both cortical domains responsible for extracting image information form spike trains (the image-forming pathway) as well as subcortical domains responsible for circadian regulation and pupillary control. In the former, the resemblance between ipGCs and a biological photometer that provides a direct readout of stimulus flux is intriguing

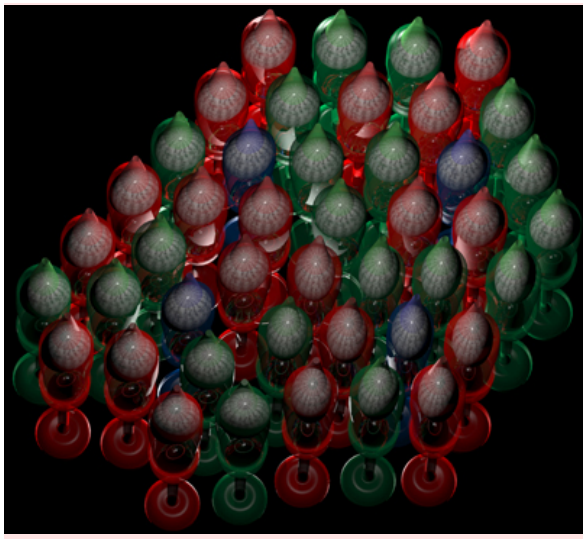

Figure 28. A patch of primate R,G,B cones.

A rendering of primate cone distributions based on the data of Marc and Sperling (Chromatic organization of primate cones. *Science*, 1977; 196:454-456). Individual cones are randomly placed but B cones make up only 7-10% of all cones. © Robert E. Marc, 2008.

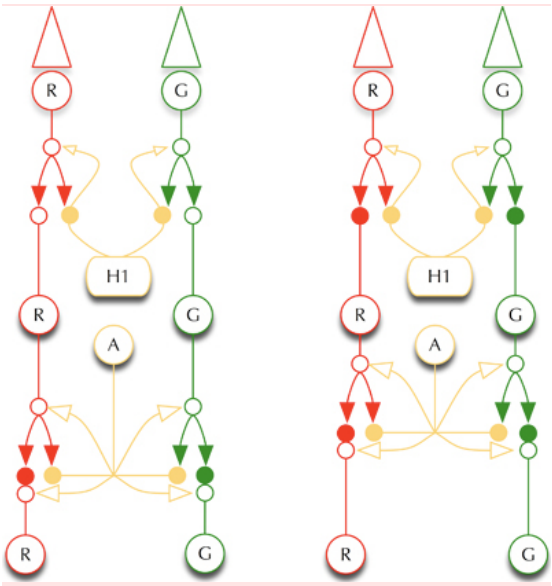

Figure 29. The midget color-opponent pathways.

Based on connectivity alone, neither the HC nor the AC surrounds appear color selective (although biased against B cones). Thus the yellow surround is always "greener" than R cones, and "redder" than G cones. © Robert E. Marc, 2008.

and may underly the psychophysical ability to gauge brightness.

RETINAL CIRCUITS UNDERLYING COLOR VISION

The cone mosaic of primates is a loose array of sparse B cones surrounded by randomly distributed R and G cones (Fig. 28). From this mosaic, all chromatic vision arises. Most mammals show evidence of dichromatic vision via opponency between B and G cones alone (166) at the GC level. This persists in primates and humans. However, since Old-world (OW) primates (Catarrhine monkeys, apes and humans) express three pigment types (R,G,B), full trichromatic vision has two spectrally opponent processes (166): (1) B/Y opponency (where the yellow signal Y is the sum of LWS$_R$ and LWS$_G$ signals) (159, 167). Roughly 30–40 million years ago, a gene duplication event in OW primates resulted in the formation of a tandem head-to-tail array of VP560 and VP530 VP genes on the primate X chromosome (10, 166). It has since been shown that LSW cones can express only one VP and selects either VP560 or VP530, creating either LWS$_R$ or LWS$_G$ expressing cones (168, 169). This is, apparently, the only gene product that differs between R and G cones. Thus there appears to be no differential molecular marker that BCs can use to select between R or G cones; no molecular marker that GCs or ACs can discern downstream to discriminate between BCs connected to R or G cones; and that the connectivity of R and G systems is probabilistic. Even so, R/G opponency is abundant in trichromatic primates.

R/G opponency. Midget BCs allow for the formation of four types of color opponency: R+/G-, R-/G+, G+/R- and G-/R+ (170). Because a chain of one LSW cone → one midget BC → one midget GC explicitly creates spectrally pure R or G cen-

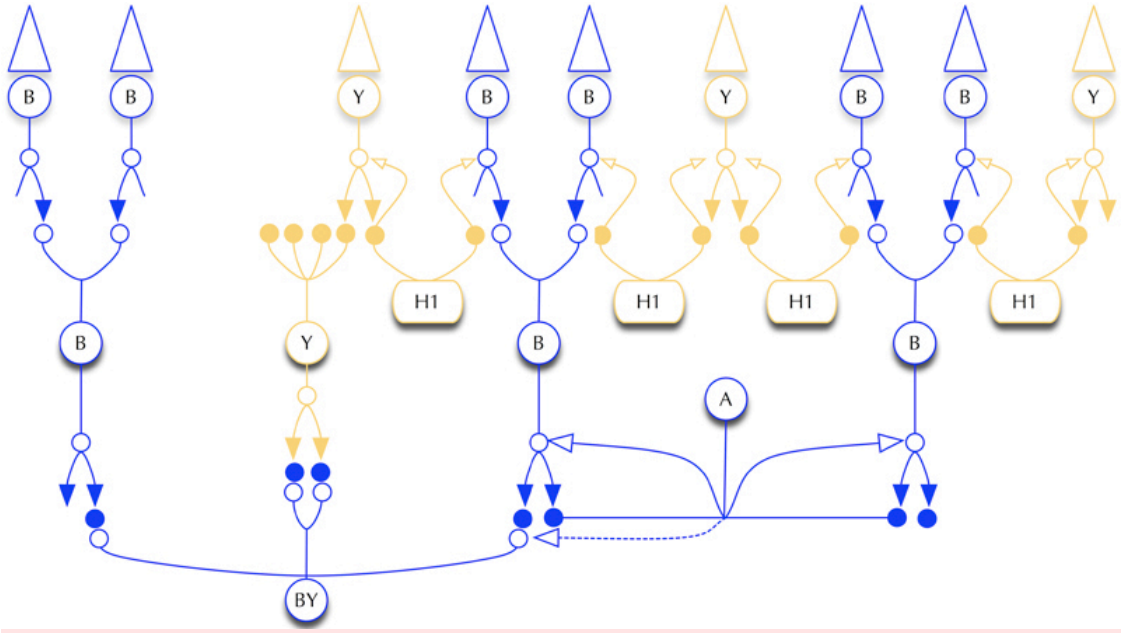

Figure 30. The blue-yellow pathways.

The BY GC has a strong blue-driven ON response and a yellow-driven OFF response. The surround arises from two possible paths: (1) Y cones → HCs → B cones or B cone BCs; (2) Y cones → OFF BCs → BY GC dendrites. © Robert E. Marc, 2008.

ter, all midget GCs will be color opponent (Fig. 29). The surround, whether derived from HCs or ACs will never be a match for the center and will always be "greener" than one R cone center or "redder" than one G cone center. Early physiological measures suggested that midget GCs with R centers had relatively "pure" G surrounds, and vice versa. Since HCs do not show any spectral selectivity for R or G cones and, in fact, sum their inputs (74), these pure surrounds could not have come via that path. Thus, it was thought that the surround organization of LSW pathways involved the selective contact of the *opponent* class of BCs by ACs forming a narrow, spectrally pure surround. Structural data show that this is not likely (171); that the AC driven surrounds of midget GCs are mixtures of R and G cones. Even so, it is clear that some midget GCs show strong R/G opponency where the surround is nearly pure (172-174). This is not consistent with the mixed-connection anatomical model. There are two possible. First, the patchiness of R and G cone distributions (21) and the small size of midget GC surrounds suggests that some midget pathways could have nearly pure opponent surrounds. Second, Lebedev and Marshak (175) developed a model network based on differential chloride gradients in midget GCs and LWSG-cone biased OFF signals, thus generating a purer R/G opponency. There is clearly much to be understood about midget GC networks, simple though they may seem on the surface. A further puzzle is why broad yellow-sensitive (Y) HC surrounds fail to dominate midget BCs, but it so clearly does so for B/Y opponent GCs . The absence of a Y surround is incompatible with a general HC $>_i$ cone feedback path affecting all BCs, including midgets (99). In their spatial summation properties, color-coded midget GCs largely resemble linear X cells. In the primate, they are

called P cells, reflecting the finding that they project to the *parvocellular* layers of the dorsal LGN (167).

B/Y opponency: The primary retinal GCs that convey blue signals are thought to be large and small bistratified B+/Y- GCs (159, 170) that collect inputs from B cone ON BCs on their distal dendrites and possibly Y inputs from diffuse OFF BCs on their distal dendrites (Fig. 30). It was originally thought that the B/Y signal generating zones were co-extensive rather than center/surround in structure, but recent findings suggest a distinct B center antagonized by a large Y surround arising from HCs via HC $>_i$ cone feedback (91). Recent anatomical evidence suggests the existence of a midget B cone OFF BC pathway (65) but how this cell would function in vision is problematic as chromatic aberration would blue the coarse B cone mosaic further at optimal focus for high resolution R and G cones. Further, putative B-/Y+ GCs have large receptive fields (161) . If all these expectations hold true, it suggests that B-/Y+ GCs are non-midget GCs with possible selectivity for midget B cone OFF BCs.

Achromatic pathways: Color vision involves more than just opponency. Hue discrimination occurs on complex backgrounds where apparent hue can shift as a function of "achromatic" brightness. And spectral environments can induce colors on white surfaces, raising the question of what neural elements subserve the percept of white as distinct from bright. Thus cells that measure reflected lights as R+G+B signals allow the visual system to encode object brightness and spectral purity. This is one role for diffuse cone BCs that, in primates, drive spectrally non-opponent parasol GCs and other wide-field GCs.

A note on the role of HCs in primate color vision: In non-mammalian vertebrates with highly developed color vision (there are many), HCs are of two kinds. In one, light of any wavelength hyperpolarizes the cell (luminosity type); in the other, some wavelengths hyperpolarize and others depolarize the cell (chromaticity type) (176). The potential relevance of chromaticity HCs for color vision in general was tantalizing and, given that color vision is pronounced in primates, it was expected that chromaticity HCs cells would be found. This turned out not to be the case, however. All HCs tested in primates hyperpolarize to any wavelength. Specifically, Dacey and coworkers found evidence for only two functional classes (74): HI cells contact all cone classes, but exhibit weak functional input from B cones. HII cells have a larger receptive fields make more B cone contacts than HI cells and receives a strong input from B cones as well as R and G cones. However, neither of these surround signals are particularly evident in midget BCs.

DIRECTIONALLY SELECTIVE (DS) GCs

DS GCs have complex trigger features: they respond to targets moving in a *preferred* direction while remaining silent when targets move in the opposite, *null* direction.(177, 178). The circuitry underlying this behavior has been partly elucidated with pharmacologic and electrophysiologic tools and involves interactions between BCs and perhaps three AC inputs, one from the starburst γ/cholinergic group and the others from two γ ACs (179). Starburst ACs have been well characterized (32, 103, 180-183): OFF starburst cells are conventional ACs that hyperpolarize to light and are driven by OFF cone BC inputs in sublamina a; ON starburst cells are displaced cells with cell bodies in the

GCL that depolarize to light and are driven by ON cone BC inputs in sublamina b. Each costratifies with a the dendrites of DS GCs and makes numerous synapses with it. The precise classes of γ ACs participating in DS GC circuits have not yet been identified, but the functional roles of GABAergic inhibition are slowly being worked out(184). One GABAergic AC inhibits the starburst ACs, whereas the other inhibits the DS GC.

The essence of the circuit is that, when stimuli come from the preferred side, a combination of excitatory glutamatergic and cholinergic signals arrives at the GC in advance of GABAergic inhibition. The notion of chained excitatory synapses suggest that pathway gain is enhanced: e.g. the BC > starburst AC > DS GC chain should have higher gain than a direct BC > GC transfer. But in the null direction, a strong GABA signal reaches the DS GC before of excitatory input and prevents it from reaching spike threshold. Blockade of inhibition with GABAA receptor antagonists prevents this effect and converts DS GCs into non-directional motion sensors (185, 186)}. Importantly, GABA inhibition is very strong even in the preferred direction and the spike responses to stimuli increase tremendously on blocking GABAergic inhibition.

DS GCs come in two classes: ON-OFF DS GCs and ON DS GCs. The former are moderately abundant in rabbit and tend to form four subclasses with preferred directions oriented in upward, downward, nasal and temporal vectors (15, 187). ON DS cells come in three subclasses with preferred directions of upper nasal, upper temporal and ventral vectors, and appear to play a role in the integration of vestibular vectors and eye movements to define the horizon (188). These classes have not been well studied in primates.

PHARMACOLOGY AND ELECTROPHYSIOLOGY OF GANGLION CELLS

The response of a GC to light is a change in membrane potential, depolarizing or hyperpolarizing, called an excitatory (EPSP) or inhibitory postsynaptic potential (EPSP, IPSP). EPSPs evoke superimposed action potentials and IPSPs inhibit firing. The waveform of postsynaptic potentials plays a large role in determining the pattern of spike firing, which may be relatively sustained or transient (145, 149, 150, 152, 189). Three factors interact to shape this waveform: cell-autonomous intrinsic voltage-gated channels in the GC membrane, cell-autonomous neurotransmitter receptor expression patterns, and cell-interactive (network) spatiotemporal patterns of excitatory (glutamatergic) and inhibitory (GABAergic and/or glycinergic) synaptic drive. Though the early work on GC pharmacology was carried out on amphibian retinas, much has now been validated in mammals.

A critical set of intrinsic voltage-gated channels in shaping GC responses are K channels (190, 191) because they determine the rate at which the membrane repolarizes after spike initiation and limit firing frequency. It is also clear that different classes of GCs express different molecular forms of voltage-gated Na channels which further shape spiking patterns. All GCs express AMPA receptors and most express a mixture of AMPA and NMDA receptors (79, 80, 192). Each family of iGluRs possesses a collection of subunit-specific properties that influence the sensitivity, amplification, kinetics and persistence of glutamate driven responses in GCs (3). In general, AMPA receptors desensitize rapidly and primarily drive fast,

transient responses. NMDA receptors are conditional receptors that require depolarization to overcome an intrinsic Mg^{++} ion block. Thus, the initial depolarization AMPA receptor activation enables a secondary NMDA receptor response. NMDA receptor kinetics are much slower than those of AMPA channels and they do not desensitize as quickly, leading to more sustained spike firing. Importantly, AMPA receptors come in a range of unitary conductance modes, with those containing the GluR2R edited subunit showing nearly 10-fold smaller currents (3). Thus AMPA receptors can mediate either fast or slow integration of EPSPs, possibly generating brisk and transient behaviors, respectively. By expressing the appropriate mixture of AMPA and NMDA receptor subtypes is possible to tune a broad spectrum of response properties.

Connections ultimately determine the polarity, broad kinetics and stimulus specificity of GCs. For example, anatomical and electrophysiologic studies indicate primate that the ratio of BC:AC synaptic contacts is higher for P- than M-stream GCs (193). Physiological analyses in amphibian retinas initially suggested that ON BCs are separable into relatively transient and relatively sustained classes, which will of course affect the time course of glutamate release by their terminals (194). Faster BCs are a natural candidate for synaptic drive for transient mammalian Y-type GCs.

GABAergic and glycinergic signaling in the mammalian retina is much less well understood in spite of the abundance of AC synapses. GCs receive both inputs and, in general, GABAergic modulation of mammalian GCs occurs through fast $GABA_A$ receptors (3). The complexity of AC synaptic networks makes the task of unraveling GABAergic/glycinergic circuitry somewhat daunting, as chains of direct AC $>_i$ AC signaling low gain constitute sign-conserving paths and pharmacologic blockade can reduce both polysynaptic excitation as well as monosynaptic inhibition. Despite the large number of feedforward and feedback paths represented by γ AC synapses, the contributions of γ ACs to GC surrounds (except for DS GCs) is problematic to extract . Both wide-field achromatic (90) and B+/Y- GCs (91) show little effect of GABAergic blockage on surround signals, suggesting that they are dominated by HCs. In retrospect, however, the effects of ACs are likely to be fast, very local and complex compared to the large, slow, simple opponent signals provided by HCs (Fig. 24). Many ACs show distinct center/surround responses with small-field spatial summation. Building networks from such cells would imply that their task is not to provide a global adaptation signal to a large unstructured background and but rather to enable fast, high-contrast discrimination of spots, edges and motion. The roles of direct gly AC > GC synapses are not well understood.

RETINAL NEUROMODULATORY SYSTEMS

Neuromodulators (195) nominally act through the intracellular biochemistry of a neuron to effect a change in function. The most common pathway for neuromodulation is through activation of GPCRs, often termed “metabotropic receptors”. Pathways downstream of activated GPCRs may facilitate, suppress, alter signal-to-noise properties, or alter kinetics of fast signaling events; may involve small molecule second messengers (cAMP, cGMP, diacylglycerol) or protein signaling chains that modulate channel function or Ca regulation.

Ligand-activated GPCRs in the retina are diverse and include group A,B,C mGluRs, $GABA_B$ receptors, mAChR, serotonin, histamine, dopamine and numerous peptide receptors (3, 119, 196, 197). Dopamine, discussed in more detail below, operates via two main receptor classes, D1 and D2. Common metabolites such as ATP and adenosine also activate membrane receptors (3), of which most are metabotropic. Peptide signaling is extremely diverse and beyond the scope of this chapter; it has been reviewed in detail by Brecha (119).

One of the most unusual and still poorly understood pathways in retinal function is the *nitrergic* system. Some neurons express high levels of nitric oxide synthase that generates nitric oxide in the process of converting arginine to citrulline (3). Some nitrergic cells are AxCs (103). Nitric oxide diffuses across cell membranes and binds to Fe residues in the heme core of soluble guanyl cyclase (198). This constitutively activates to cyclase to generate high cGMP levels which, in turn, modulates gap junction permeability(49) and opens nearby CNG channels. How these systems are normally activated and why they are invoked is not clear. Further, many cells other than AxCs are suspected to generate nitric oxide (198).

Neuromodulators tend to act on long time scales (seconds to minutes) and influence global rather than merely local functions. Every retinal neuron has multiple GPCRs and other response elements in addition to its ionotropic receptors, from which it follows that each neuron undergoes continuous fine-tuning, with each of its voltage-sensitive, ligand-gated, and gap junctional channels subject to modulation. The process of neurotransmitter release is also sculpted by neuromodulatory influences (197).

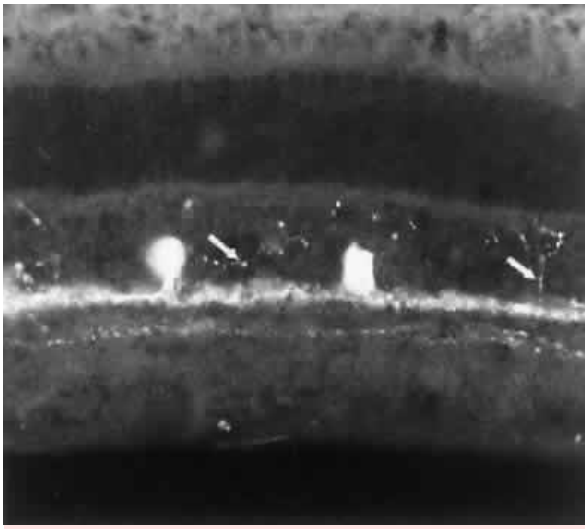

Figure 31. Dopaminergic neurons of the retina revealed by anti-TH IgGs.

Two immunoreactive dopaminergic neuronal perikarya are seen at the border of the inner nuclear layer and the inner plexiform layer. Their dendrites extend primarily as a horizontal sheet in the distalmost portion of the inner plexiform layer, but occasional processes (arrows) pass through the inner nuclear layer to end in the vicinity of the OPL. (Unpublished data of R. Gabriel and P. Witkovsky; × 600)

DOPAMINE: A MODEL NEUROMODULATOR

Dopamine is by far the best understood neuromodulator. Dopaminergic retinal neurons are found throughout the vertebrates as AxCs and/or interplexiform cells (3, 199, 200), with large somas sparsely distributed at 10 to 50 cells/mm^2. In mammals, class TH1 (tyrosine hydroxylase type 1) AxCs, are narrowly stratified cells that arborize at level 0–10 of the inner plexiform layer (Fig. 31) with medium-field dendritic arbors and fine, complex axon terminal fields (201). Despite this location in the OFF sublamina, recordings from TH1 cells in mouse show them to be ON cells (202). At the same time, GABAergic blockade picrotoxin or bicuculline evokes

strong dopamine release (203-205). This suggests that one pathway for light-dependent drive is OFF BC > γ ACs >$_i$ TH1 AxCs. However, $GABA_A$ antagonists do not appear to block light responses (202) and TH1 cells possess weak AMPA and moderate NMDA drive (206), suggesting direct BC input (207). Hokoc and Mariani (207) further argued the BC input arose from giant bistratified BCs, which may in fact be ON center cells. This suggests that parallel OFF and ON BCs drive TH1 AxCs paths with a net ON polarity.

Dopaminergic AxCs are extremely potent. First, most or all retinal neurons, express D1 and/or D2 receptors, and in many cases dopamine reaches these receptors by diffusion rather than through a morphologically defined synapse (3, 200, 208). This is an example of volume transmission, once applied principally to blood-borne hormones but now known to occur throughout the nervous system. In the case of dopamine, the diffusion distances may be tens of microns (208, 209). The second organizational principle of dopaminergic AxCs is that synthesis and release are coupled in an on-demand system (210). When dopamine release is activated, more is synthesized. This regulation occurs partly by phosphorylation (211). TH, the rate-limiting enzyme for dopamine synthesis, has phosphorylation sites at S19, S31, and S40, modified according to the activity of the neuron (212). However, even when isolated from all synaptic drive, TH1 AxCs appear to be spontaneously spiking 'pacemaker' cells that resemble spontaneously signaling dopamine neurons in brain (213, 214). The presence of weak excitatory inputs suppressed by many inhibitory inputs suggests that it takes a relatively small depolarization to escape from inhibition. Further, TH1 cells appear to be activated by dawn, and dopamine diffuses through the retina to its various targets (215). Basically, dopamine signals light-adapt the retina by GPCR-coupled processes: e.g., dopamine-activated D1 receptors → adenyl cyclase activation → increased $[cAMP]_i$ → protein kinase A (PKA) activation (216). PKA signaling in different cell classes evokes different effector events such as HC and AC uncoupling (217, 218) and modulated spike train duration.(219). In addition, TH1 AxCs display the largest complement of circadian clock genes of any retinal cell (220-222) and appear to anticipate dawn, thus setting retina up for photopic function. Dopamine also modulates melatonin production by photoreceptors (223) and thus indirectly controls dawn-activated disk shedding by rods (224). Dopamine has even been implicated in eye growth in relation to myopia, although the pathway by which this regulation might occur is still quite unclear.

In a novel finding, the dendrites of TH1 AxCs appear to co-fasciculate with those of melanopsin-expressing ipGCs (225) and there is the suggestion that they may modulate or even drive ipGCs (206, 226) or vice- versa (227). An additional complication of TH1 cell behavior and connectivity is that, like nigrostriatal DA neurons (228), retinal TH1 AxCs possess molecular signatures of glutamatergic neurons (206). Thus they could pass their ON responses directly to the dendrites of ipGCs via iGluRs. Given the very sustained spike patterns of isolated TH1 AxCs and their likely sluggish-sustained response profile, they are well-placed to drive the network portion of the ipGC intensity response curve (161).

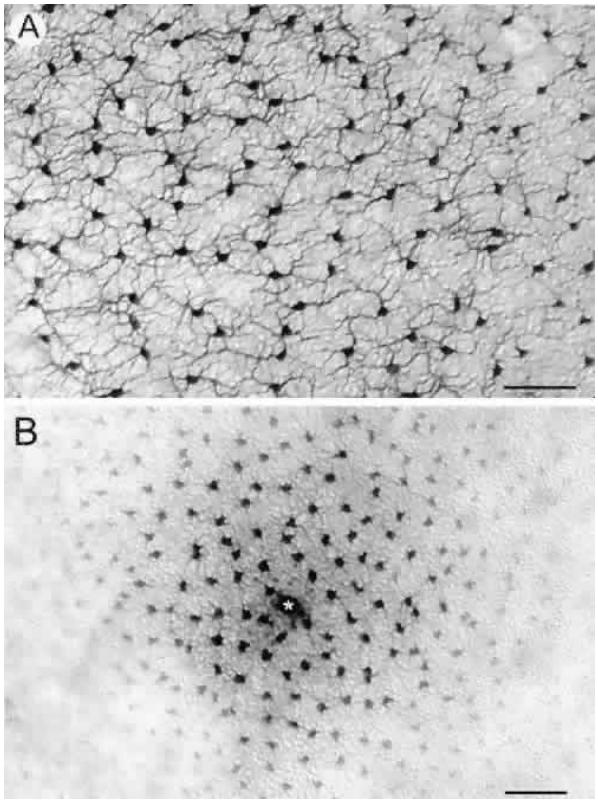

Figure 32. Neurobiotin coupling among HCs of the rabbit retina.

A. Tracer-coupled A-type HCs cells in the dark-adapted rabbit retina after injection of Neurobiotin into a single cell. The micrograph shows only a portion of the network, which comprised more than 1,000 cells extending 2,350 µm across the axis parallel to the visual streak. B. Tracer-coupled B-type HCs in the dark-adapted rabbit retina. This network included 227 cells extending 400 µm along the axis parallel to the visual streak. The asterisk indicates the point of injection. Scale bars are 50 µm. (Xin D, Bloomfield SA: Dark- and light-induced changes in coupling between HCs in the rabbit retina. J Comp Neurol 383:512, 1998, with permission of the authors and Wiley-Liss).

GAP JUNCTIONS IN THE RETINA AND THEIR MODULATION BY DOPAMINE

Many classes of retinal cells are coupled by gap junctions (42). Coupling can occur between cells of the same class (homocellular coupling): e.g. RPE cells, HCs (Fig. 32), LWS cones, gly AII rod ACs, γ rod ACs. It can also occur *across* classes (heterocellular coupling): rod::cone, gly rod AC::ON cone BC, γ AC::GC. The dominant connexins in retina are Cx36 expressed by photoreceptors, as well as Cx 45 and Cx 36 expressed BCs and certain ACs; and Cx 50/57 in HCs (229, 230). There are many more expressed at lower levels and connexin type-mixing to produce heterotypic gap junctions occurs, especially in heterocellular coupling. The connexin type influences both conductance and modifiability. The best known modulation is HC connexin conductance control via D1 dopamine receptors. First defined in fish (231) and turtle (232), it has been shown subsequently that mammalian HC connexins are under similar control (218). HCs express D1 receptors that behave as described above, leading to PKA activation and presumed connexin phosphorylation. Strong evidence for this has been obtained in zebrafish (233). The net effect is to decrease gap junction conductance so that spread of current from distant HCs is attenuated. This reduces the size of the HC-driven surround but also enhances it locally, potentiating feedback near target BCs and sharpening the tuning of photopic RFs. Another pathway for modulation of gap junction conductance is through nitric oxide as mentioned above (234). Although both nitric oxide and dopamine reduce gap junction coupling, they act through different AxCs which may have visual different thresholds. HC uncoupling is also induced by retinoic acid (RA) (235), a metabolite of the visual cycle that may be produced in the RPE. Whether significant retinoic acid levels are ever achieved in the neural retina or within HCs remains unknown, as does the mechanism of uncoupling. RA normally acts through slow transcriptional regulation and so any fast, direct action on gap junctions might be epiphenomenal. Rod-cone gap junctions also are modulated by dopamine in non-mammalians (236) but through a D2 re-

ceptor → A leading to a presumed AC activity decrease → cAMP drop (assuming a constant phosphodiesterase activity), effecting increased rod::cone coupling. The phenomenon has not been documented in mammalian photoreceptors, although mouse rods do express the D4 subclass of the D2 receptor family whose activation inversely modulates phosducin phosphorylation in mouse rods (237).

As dopamine release appears strongly associated with the scotopic → photoptic transition, one might expect dopamine to influence coupling of other neurons in the rod pathway. Indeed, dopamine appears to decrease homocellular AII AC::AII AC coupling (217) and nitric oxide acts through cGMP to decrease heterocellular gly rod AC::cone BC coupling (49), but the quantitative relationship between adaptation states and dopamine requires further characterization.

RETINAL GLIAL CELLS

MCs are the principal glial cell of the retina and comprise more of its mass than any other single cell class (93). Their functions have been reviewed in many publications and involve a literature so large it would double the reference list. MCs are large cells (Fig. 1) with somas positioned in mid-INL and radial processes that seal the neural retina from all extraretinal substrate sources on the photoreceptor, vitreal and vascular faces. Specifically, MCs form homocellular intermediate junctions at their end feet, creating a high-resistance seal between the neural retina and the vitreous. At their distal microvillar endings, they form mixed hetero-homocellular intermediate junctions with themselves and photoreceptors, sealing the subretinal space between the RPE and the external limiting membrane. Internally the fine processes of MCs surround the endothelia of capillaries and form intermediate junctions, creating a true internal blood-retinal barrier. MCs have a vast number of established and suspected functions, making them one of the most complex eukaryote cells known:

- Blood-retinal-barrier formation via intermediate junctions
- Blood retinal barrier induction of endothelium tight junctions
- Contribution to the extracellular matrix of basement membranes
- $[K^+]_o$ regulation via differential somatic and K^+ channel expression
- $[Glutamate]_o$ regulation via SLC1A3 (EAAT1) transport
- $[GABA]_o$ regulation via SLC6A13 (GAT2) transport
- Glutamate → Glutamine recycling via GS
- GABA → Glutamate recycling via GABA transaminase
- Transretinal water transport via aquaporin4
- Osmoregulatory control via taurine fluxes
- Transcellular glucose transport (endothelia → MCs → neurons)
- DA1 receptor-activated glycogenolysis
- Reactive-oxygen species regulation via glutathione production
- Retinoid cycling
- Stress/swelling/inflammatory protective responses
- Vascular flow regulation via ATP release
- Potential generation of neural progenitor cells

Three homeostatic roles in particular have been well-documented. The first is the regulation of $[K]_o$ (238). When neurons are depolarized they release K^+ into the extracellular space. Neurons have their own Na^+/K^+ exchangers to restore ion balances but are aided by MCs highly permeable to K^+ acting as sinks, particularly in the inner portion of the cell. The result is a circuit whereby K^+ from the extracellular space enters the MC and is moved into the vitreous body via efflux through the end feet. A second process is SLC1A3 Na^+-dependent transporter-mediated removal of glutamate overflow after its release at photoreceptor

and BC synapses (239, 240) as described earlier. In particular, glutamate released from synaptic vesicles in the dark must diffuse through a complex path past the dendrites of HCs and BCs, as well as past cone SLC1A2 or rod SLC1A7 transporters. Indeed, the action of glutamate on distant KA receptors of OFF BCs demonstrates that significant glutamate must always overflow to reach MCs, and without such transport buffering all cells would be depolarized in light as first shown by Ishida and Fain via transporter blockade with D-Asp (241). Finally, MCs are critical for recycling carbon skeletons accumulated via glutamate and GABA transport (3, 242-244). MCs are also responsive to glutamate (245) , dopamine and peptides (246), and growth factors (247). The significance of this sensitivity is unknown and indeed NMDA-activated currents in MCs must be at least 10-fold smaller than in neurons (79), although one may speculate that such small currents keep MCs locally informed about neuronal activity and perhaps regulate K^+ and glutamate clearance.

A second neuroglial class, astrocytes (AsCs), is present in the optic nerve (248). AsCs participate in transcellular Ca^{2+} waves, which can be stimulated by mechanical activity. Ca^{2+} waves have been shown to inhibit the activity of nearby retinal GCs (249) , an action postulated to depend on stimulation of inhibitory interneurons by glutamate released from glia. In addition, ATP release by MCs can modulate neural function (250). Like the MCs cells, AsCs are coupled to each other and to MCs. The heterocellular coupling, however, appears to be unidirectional MC→AsC. In any event, these two glial classes communicate and can interact in regulating neuronal function. Importantly, recent evidence suggests that AsCs are agents in stress over-activation of inflammatory responses in glaucoma that leads to local axonal damage within the optic nerve head (251, 252). It is very probable that Ca^{2+} signaling plays a role in this process.

OVERVIEW

This essay has attempted to provide a broad review of retinal neurons, their connections and their functional properties, and homeostasis in relation to information processing by the retina. To return to Ramón y Cajal's essential perception: the retina is a piece of the central nervous system organized into microcircuits, which he deciphered based solely on anatomical criteria. Given the absence of functional data, and that important concepts such as the (i) molecular bases of synaptic and coupling-based signaling, (ii) Shannon's laws of information flow, and (iii) formal network control theory were yet decades away, it is not surprising that Ramón y Cajal had great difficulties with HCs and ACs, whose anatomies provided no clue to the direction of signal propagation. From a modern vantage, we now understand conclude that the microcircuits of the mammalian retina reduce the visual information to a set of some 15-20 filtered versions biased for contrast, color, form and motion.

It is also important to realize that the retina is a tonic signal processor and neuroendocrine machine. Both rod and cones release glutamate at a high rate in darkness, leading to tonic spiking in darkness by many GCs. Global retinal activity is also subject to circadian control through a pacemakers possibly located in the photoreceptor cells (253) or TH1 cells (220-222), and further modified by a smoothly changing diurnal ambient light levels. We now appreciate that many micronetworks and neuroactive

agents in the retina are both influenced by and signal these changes, including melatonin and dopamine release (254), to name only the best studied of these. Many activities of the retina appear to be diurnal or even circadian, including disk shedding by rods and the sensitivity of the photoreceptors. The fast circuits that respond to rapid light signals serving pattern vision, color perception, and motion detection function against a background of slower changes that set the tone of the system through neuromodulation: slower pathways that influence the state of the hardwired circuits.

In addition to our incomplete but expanding view of the basic complexity of retinal circuitry, it is now clear that the mammalian retina is not static. In fact, the mammalian retina displays complex postnatal synaptic refinement (255, 256) similar to the CNS, including revisions in gene expression in response to visual environments at maturity (257, 258), and reactive rewiring when challenged by photoreceptor degenerations (88, 259, 260). The scope and underlying mechanisms of these changes remain unknown, but adult retinal neurons can clearly revise patterns of synaptic contacts as well as generate new processes and synapses. During postnatal life in rodents, the visual environment influences the onset of bouts of spontaneous signaling thought to be required for synaptic maturation (256) and modulates the segregation of the inner plexiform layer into ON and OFF sublayers, apparently through a dendritic pruning process (261). In addition to these developmental and adult plasticities, and extensive repertoire of outer retinal changes are triggered by retinal detachment, including neurite sprouting, neuronal migration and MC hypertrophy (262).

The details and subtleties of these issues are far more complex than can be glossed here, but it is fair for a clinician-scientist interested in translational research to ask why we must be obsessed with such details? There are three answers. First, one cannot discard information as unimportant until you have it. Indeed, the first visual defect in some forms of retinitis pigmentosa is likely to be a synaptic and even molecular disconnection between photoreceptors and BCs long before the first rod dies (88). Understanding this process begins with a full explication of the molecular biology of mGluR and iGluR systems, classically beyond the clinical purview. Second, our newest tools have challenged simple views of retinal function by finding new neurons, new connections and new functionalities in the retina. The ipGC is only one of these (157). For example, molecular detection strategies and gene expression screens now reveal complex heterocellular events in retinal disease (263), often involving both neural retina and even optic nerve (252, 264). Third, understanding microcircuitry has enabled us to belatedly discover that retinal degenerations once viewed as restricted to the outer retina are progressive, and invade the neural retina. Understanding the fine-scale molecular rules underlying this pathologic remodeling will be essential to any true attempt to restore vision in advanced retinitis pigmentosa, AMD, glaucoma and vasculopathies. The next frontier for functional retinal neuroanatomy is understanding how vision is built from circuits and how disease-activated remodeling corrupts circuits, and to design molecular, cellular or solution to these new challenges.

ACKNOWLEDGMENTS

This revised work was supported by NIH grants NEI R01 EY02576, R01 EY015128, and the Cal and JeNeal Hatch Presidential Endowed Chair (REM). I especially thank Dr. Paul Witkovsky who crafted the original framework for this chapter. I have retained much of it as I could not improve it. Again, this new version owes thanks to Drs. S. Bloomfield, S. Haverkamp, D. Krizaj, R. Masland, P. Sterling, and their publishers for permitting the reproduction of figures from their published work. Dr. Helga Kolb is owed special thanks for allowing use of five unpublished figures.

REFERENCES

1. Ramón y Cajal S. *The Structure of the Retina*. Springfield, IL: Charles C. Thomas. 1972.
2. Levitan IB. Modulation of ion channels by protein phosphorylation and dephosphorylation. *Annu Rev Physiol*, 1994;56:193-212.
3. Marc RE. Retinal Neurotransmitters. In: Chalupa LM, Werner J, Eds. *The Visual Neurosciences*, Cambridge, MA: MIT Press, 2004:315-330.
4. Fuxe K Agnati LF. *Volume Transmission in the Brain*. Advances in Neuroscience. Vol. 1. New York: Raven Press. 1991.
5. Polyak S. *The Retina*. Chicago: University of Chicago Press. 1941.
6. Morgan JL, Dhingra A, Vardi N*, et al.* Axons and dendrites originate from neuroepithelial-like processes of retinal bipolar cells. *Nat Neurosci*, 2006;9:85–92.
7. Marc RE. Functional Neuroanatomy of the Retina. In: Albert D, Miller J, Eds. *Albert and Jakobiec's Principles and Practice of Ophthalmology*. Elsevier, 2008;1565-1592.
8. Gupta N, Brown KE, Milam AH. Activated microglia in human retinitis pigmentosa, late-onset retinal degeneration, and age-related macular degeneration. *Exp Eye Res*, 2003;76:463-471.
9. Harada T, Harada C, Kohsaka S*, et al.* Microglia-Muller glia cell interactions control neurotrophic factor production during light-induced retinal degeneration. *J Neurosci*, 2002;22:9228-9236
10. Nathans J. The evolution and physiology of human color vision: insights from molecular genetic studies of visual pigments. *Neuron*, 1999;24:299–312.
11. Gullapalli VK, Sugino IK Zarbin MA, Müller cells and the retinal pigment epithelium. in Albert D. Miller J, Eds. *Albert and Jakobiec's Principles and Practice of Ophthalmology*. Elsevier, 2008;addpages.
12. Ochs M, Mayhew TM Knabe W. To what extent are the retinal capillaries ensheathed by Müller cells? A stereological study in the tree shrew *Tupaia belangeri. J. Anat.*, 2000;196: 453–461.
13. Ambati BK, Nozaki M, Singh N*, et al.* Corneal avascularity is due to soluble VEGF receptor-1. *Nature*, 2006;443(7114):993-997.
14. Yannuzzi LA, Negrão S, Iida T*, et al.* Retinal angiomatous proliferation in age-related macular degeneration. *Retina*, 2001;21:416-434.
15. Oyster C. *The Human Eye*. New York: Sinauer. 1999.
16. Bayer BE. *Color imaging array*. 1976: US Patent 3971065
17. Marc RE. Chromatic patterns of cone photoreceptors. 1976 Glenn A. Fry Award Lecture. *Am J Optometry & Physiolog Optics*, 1977; 54(4):212-225.
18. Marc RE Sperling HG. Color receptor identities of goldfish cones. *Science*, 1976; 191:487-489.
19. Marc RE Sperling HG. Chromatic organization of primate cones. *Science*, 1977; 196:454-456.
20. Curcio CA, Allen KA, Sloan KR*, et al.* Distribution and morphology of human cone photoreceptors stained with anti-blue opsin. *J Comp Neurol*, 1991;312:610–624.
21. Hofer H, Carroll J, Neitz J*, et al.* Organization of the human trichromatic cone mosaic. *J Neurosci* 2005;25:9669-9679.
22. Curcio CA, Sloan KR, Kalina RE*, et al.* Human photoreceptor topography. *J Comp Neurol*, 1990;292:497-523.
23. Jeon CJ, Strettoi E Masland RH. The major cell populations of the mouse retina. *J Neurosci*, 1998;18:8936-46.

24. Wässle H Riemann HJ. The mosaic of nerve cells in the mammalian retina. *Proc Roy Soc London - B*, 1976; 200:441-462.
25. Reese B. Mosaics, tiling and coverage by retinal neurons. In: Masland RH, Albright T, Eds. *The Senses: A comprehensive reference. Vision*. Amsterdam: Elsevier, 2008;439-456.
26. Engstrom K, Ahlbert IB. Cone types and cone arrangement in the retina of some flatfishes. *Acta Zool*, 1963; 44:1–11.
27. Van Haesendonck E, Missotten L. Patterns of glutamate-like immunoreactive bipolar cell axons in the retina of the marine teleost, the dragonet. *Vision Research*, 1991;31:451-462.
28. Kalloniatis M, Marc RE. Interplexiform cells of the goldfish retina. *J Comp Neurol*, 1990;297:340-58.
29. Cook JE. Spatial properties of retinal mosaics: an empirical evaluation of some existing measures. *Vis Neurosci*, 1996;13:15-30.
30. Kolb H, Linberg KA, Fisher SK. Neurons of the human retina: a Golgi study. *J Comp Neurol*, 1992;318:147-187.
31. Dacey DM. The mosaic of midget ganglion cells in the human retina. *J Neurosci*, 1993;13:5334.
32. Tauchi M, Masland RH. The shape and arrangement of the cholinergic neurons in the rabbit retina. *Proc R Soc Lond B*, 1984;223:101-119.
33. Crook JM, Lange-Malecki B, Lee BB*, et al*. Visual resolution of macaque retinal ganglion cells. *J Physiol Lond*, 1988;396:205-224.
34. Matthews G. Synaptic mechanisms of bipolar cell terminals. *Vision Research*, 1999;39:2469-76.
35. Wilson M. Retinal Synapses. In: Chalupa LM, Werner J, Eds. *The Visual Neurosciences*. Cambridge, MA: MIT Press, 2004; 279–303.
36. Llinas R, Sugimori M, Silver RB. The concept of calcium concentration microdomains in synaptic transmission. *Neuropharmacology*, 1995;34:1443-1451.
37. Golovina VA, Blaustein MSpatially and functionally distinct Ca2+ stores in sarcoplasmic and endoplasmic reticulum. *Science*, 1998;275:1643-1648.
38. Szikra T, Krizaj D. Intracellular organelles and calcium homeostasis in rods and cones. *Vis Neurosci*, 2007;24:733-743.
39. Chang B, Heckenlively JR, Bayley PR*, et al*. The nob2 mouse, a null mutation in Cacna1f: anatomical and functional abnormalities in the outer retina and their consequences on ganglion cell visual responses. *Vis Neurosci*, 2006;23:11-24.
40. Goodenough DA. Bulk isolation of mouse hepatocyte gap junctions. *J Cell Biol*, 1974; 61:557-563.
41. Guldenagel M, Sohl G, Plum A*, et al*. Expression patterns of connexin genes in mouse retina. *J Comp Neurol*, 2000;425:193-201.
42. Massey SC. Circuit functions of gap junctions in the mammalian retina. In: Masland RH, Albright T, Eds. *The Senses: A comprehensive reference. Vision*. Amsterdam: Elsevier, 2008;457-471.
43. Mills SL, Massey SC. A series of biotinylated tracers distinguishes three types of gap junction in retina. *J Neurosci*, 2000;20:8629-36.
44. Mills SL, O'Brien JJ, Li W*, et al*. Rod pathways in the mammalian retina use connexin 36. *J Comp Neurol*, 2001;436:336-50.
45. Feigenspan A, Teubner B, Willecke K*, et al*. Expression of neuronal connexin36 in AII amacrine cells of the mammalian retina. *J Neurosci*, 2001;21:230-9.
46. Lin B, Jakobs TC, Masland RH, Different functional types of bipolar cells use different gap-junctional proteins. *J. Neurosci* 2005;25:6696-6701.
47. Raviola E, Gilula NB. Gap junctions between photoreceptor cells in the vertebrate retina. *Proc Natl Acad Sci U S A.*, 1973; 70:1677-1681.
48. Mills SL, Massey SC. Distribution and coverage of A- and B-type horizontal cells stained with Neurobiotin in the rabbit retina. *Vis Neurosci*, 1994;11:549-560.
49. Mills SL, Massey SC. Differential properties of two gap junctional pathways made by AII amacrine cells. *Nature*, 1995;377:734-737.
50. Bloomfield SA, Xin D. A comparison of receptive-field and tracer-coupling size of amacrine and ganglion cells in the rabbit retina. *Vis Neurosci*, 1997;14:1153-1165.

51. Rao-Mirotznik R, Buchsbaum G, Sterling Transmitter Concentration at a Three-Dimensional Synapse. *J Neurophysiol*, 1998;80:3163-3172.
52. Rao-Mirotznik R, Harkins AB, Buchsbaum G, *et al.* Mammalian rod terminal: Architecture of a binary synapse. *Neuron*, 1995;14:561-569.
53. Sterling How retinal circuits optimize the transfer of visual information. In: Chalupa LM, Werner J, Eds. *The Visual Neurosciences*. Cambridge, MA: MIT Press, 2004;234–259.
54. Perkins GA, Ellisman MH, Fox DA, Three-dimensional analysis of mouse rod and cone mitochondrial cristae architecture: bioenergetic and functional implications. *Mol Vis*, 2003;9:60-73.
55. Migdale K, Herr S, Klug K, *et al.* Two ribbon synaptic units in rod photoreceptors of macaque, human, and cat. *J Comp Neurol*, 2003;455:100-112.
56. Chun M-H, Grünert U, Martin PR, *et al.* The synaptic complex of cones in the fovea and in the periphery of the macaque monkey retina. *Vision Research*, 1996;36:3383-3395.
57. Schmitz Y, Witkovsky P. Dependence of photoreceptor glutamate release on a dihydropyridine-sensitive calcium channel. *Neuroscience*, 1997;78:1209-1216.
58. Wilkinson MF, Barnes S. The dihydropyridine-sensitive calcium channel subtype in cone photoreceptors. *J Gen Physiol*, 1996;107:621-630.
59. Szikra T, Krizaj D,.The dynamic range and domain-specific signals of intracellular calcium in photoreceptors. *Neuroscience*, 2006;141:143-155.
60. Johnson JEJ, Perkins GA, Giddabasappa A, *et al.* Spatiotemporal regulation of ATP and Ca2+ dynamics in vertebrate rod and cone ribbon synapses. *Mol Vis*, 2007;13:887-919.
61. Krizaj D. Compartmentalization of calcium entry pathways in mouse rods. *European J Neurosci*, 2005;22:3292-3296.
62. MacNeil MA, Huessy JK, Dacheux RF, *et al*. The population of bipolar cells in the rabbit retina. *The J Comp Neurol*, 2004;472:73-86.
63. Kolb H, Marshak DW. The midget pathways of the primate retina. *Doc Ophthalmol*, 2003;106:67–81.
64. Lee SCS, Telkes I, Grunert U. S-cones do not contribute to the OFF-midget pathway in the retina of the marmoset, Callithrix jacchus. *European J Neurosci*, 2005:437-447.
65. Klug K, Herr S, Ngo IT, *et al.* Macaque retina contains an S-Cone OFF midget pathway. *J Neurosci*, 2003;23:9881-9887.
66. Kouyama N, Marshak DW. Bipolar cells specific for blue cones in the macaque retina. *J Neurosci*, 1992;12:1233-1252.
67. Liu P-C, Chiao C-C. Morphologic Identification of the OFF-Type blue cone bipolar cell in the rabbit retina. *Invest Ophthalmol Vis Sci* 2007;48:3388-3395.
68. Lee SCS, Grunert U. Connections of diffuse bipolar cells in primate retina are biased against S-cones. *J Comp Neurol*, 2007;502:126-140.
69. Li W, DeVries SH. Bipolar cell pathways for color and luminance vision in a dichromatic mammalian retina. *Nat Neurosci*, 2006;9:669-675.
70. Dacheux RF, Raviola E. Horizontal cells in the retina of the rabbit. *J Neurosci* 1982;2:1486–1493
71. Raviola E, Dacheux RF. Variations in structure and response properties of horizontal cells in the retina of the rabbit. *Vision Research*, 1983;23:1221–1227.
72. Perlman I, Kolb H, Nelson R. Anatomy, circuitry, and physiology of vertebrate horizontal cells. In: Chalupa LM, Werner J, Eds. *The Visual Neurosciences*. Cambridge, MA: MIT Press, 2004;369–394.
73. Nelson R. Cat cones have rod input: a comparison of the response properties of cones and horizontal cell bodies in the retina of the cat. *J Comp Neurol*, 1977; 172:109–136.
74. Dacey DM, Lee BB, Stafford DK, *et al.* Horizontal cells of the primate retina: cone specificity without spectral opponency. *Science*, 1996;271:656-659.
75. Kolb H, Fernandez E, Schouten J, *et al.* Are there three types of horizontal cell in the human retina? *J Comp Neurol*, 1994;343:370-386.
76. Packer OS, Dacey DM. Synergistic center-surround receptive field model of monkey

H1 horizontal cells. *J Vision*, 2005;5:1038–1054.
77. Wässle H, Dacey DM, Haun T*, et al*. The mosaic of horizontal cells in the macaque monkey retina: with a comment on biplexiform ganglion cells. *Vis Neurosci*, 2000;17:591-608.
78. Gustafson EC, Stevens ER, Wolosker H*, et al*. Endogenous D-Serine contributes to NMDA-receptor-mediated light-evoked responses in the vertebrate retina. *J Neurophysiol,* 2007;98:122-130.
79. Marc RE. Mapping glutamatergic drive in the vertebrate retina with a channel-permeant organic cation. *J Comp Neurol*, 1999;407:47-64.
80. Marc RE. Kainate activation of horizontal, bipolar, amacrine, and ganglion cells in the rabbit retina. *J Comp Neurol*, 1999;407:65-76.
81. Blanco R, de la Villa P. Ionotropic glutamate receptors in isolated horizontal cells of the rabbit retina. *European J Neurosci*, 1999;11:867-73.
82. Pan F, Massey SC. Rod and cone input to horizontal cells in the rabbit retina. *The J Comp Neurol*, 2007;500:815-831.
83. DeVries SH, Li W, Saszik S. Parallel processing in two transmitter microenvironments at the cone photoreceptor synapse. *Neuron*, 2006;50(5):735-748.
84. Dhingra A, Lyubarsky A, Jiang M*, et al*. The light response of ON bipolar neurons requires Gαo. *J Neurosci*, 2000;20:9053-9058.
85. Gaal l, Roska B, Picaud SA*, et al*. Postsynaptic response kinetics are controlled by a glutamate transporter at cone photoreceptors. *J Neurophysiol*, 1998;79:190-196.
86. Tsukamoto Y, Morigiwa K, Ishii M*, et al*. A novel connection between rods and ON cone bipolar cells revealed by ectopic metabotropic glutamate receptor 7 (mGluR7) in mGluR6-deficient mouse retinas. *J Neurosci*, 2007;27:6261-6267.
87. Hanna MC, Calkins DJ. Expression of genes encoding glutamate receptors and transporters in rod and cone bipolar cells of the primate retina determined by single-cell polymerase chain reaction. *Mol Vis*, 2007;13:2194-2208.
88. Marc RE, Jones BW, Anderson JR*, et al*. Neural reprogramming in retinal degenerations. *Invest Ophthalmol Vis Sci*, 2007;48:3364-3371.
89. Dacey DM, Packer OS, Diller L*, et al*. Center surround receptive field structure of cone bipolar cells in primate retina. *Vision Research*, 2000;40:1801-1811.
90. McMahon MJ, Packer OS, Dacey DM. The classical receptive field surround of primate parasol ganglion cells is mediated primarily by a non-GABAergic pathway. *J Neurosci* , 2004;24:3736-3745.
91. Field GD, Sher A, Gauthier JL*, et al*. Spatial properties and functional organization of small bistratified ganglion cells in primate retina. *J Neurosci*, 2007;27:13261-13272.
92. Marc RE. Structural organization of GABAergic circuitry in ectotherm retinas. *Progress in Brain Research*, 1992;90:61-92.
93. Kalloniatis M, Marc RE Murry RF. Amino acid signatures in the primate retina. *J Neurosci*, 1996;16:6807-29.
94. Picaud S, Pattnaik B, Hicks D*, et al*. GABAA and GABAC receptors in adult porcine cones: evidence from a photoreceptor-glia co-culture model. *J Physiol*, 1998;513:33-42.
95. Enz R, Brandstatter JH, Wässle H*, et al*. Immunocytochemical Localization of the GABAC Receptor *rho* subunits in the mammalian retina. *J Neurosci*, 1996;16:4479-4490.
96. Vardi N, Zhang L-L, Payne JA*, et al*. Evidence that different cation chloride cotransporters in retinal neurons allow opposite responses to GABA. *J Neurosci*, 2000;20:7657–7663.
97. Kamermans M, Fahrenfort I. Ephaptic interactions within a chemical synapse: hemichannel-mediated ephaptic inhibition in the retina. *Curr Opin Neurobiol*, 2004;14:531-541.
98. Good NE, Winget GD, Winter W*, et al*. Hydrogen ion buffers for biological research. *Biochemistry*, 1966; 5:467-477.
99. Davenport CM, Detwiler PB, Dacey DM. Effects of pH buffering on horizontal and ganglion cell light responses in primate retina: evidence for the proton hypothesis of surround formation. *J Neurosci*, 2008;28:456-464.

100. Baylor DA, Fuortes MGF, O'Bryan PM. Receptive fields of cones in the retina of the turtle. *J Physiol*, 1971; 214:265-294.
101. Fuortes MGF, Schwartz EA, Simon EJ. Colour-dependence of cone responses in the turtle retina. *J Physiol*, 1973; 234:199-216.
102. Naka K-I, Witkovsky. Dogfish ganglion cell discharge resulting from extrinsic polarization of the horizontal cells. *J Physiol*, 1972; 223(2):449-460.
103. Vaney DI. Retinal amacrine cells. In: Chalupa LM, Werner J, Eds. *The Visual Neurosciences*, Cambridge, MA: MIT Press, 2004: 395-409.
104. MacNeil MA, Heussy JK, Dacheux RF*, et al*. The shapes and numbers of amacrine cells: matching of photofilled with Golgi-stained cells in the rabbit retina and comparison with other mammalian species. *J Comp Neurol*, 1999;413:305-26.
105. Wilson M, Vaney DI. Amacrine cells. in Masland RH, Albright T, Eds. *The Senses: A comprehensive reference. Vision.* Amsterdam: Elsevier, 2008;361-367.
106. Haverkamp S Wässle H. Immunocytochemical Analysis of the Mouse Retina. *J Comp Neurol*, 2000;424:1-23.
107. Kolb H,.Amacrine cells of the mammalian retina: neurocircuitry and functional roles. *Eye*, 1997;11:904-923.
108. Bloomfield SA, Völgyi B. Response properties of a unique subtype of wide-field amacrine cell in the rabbit retina. *Vis Neurosci*, 2007;24:459-469.
109. Völgyi B, Xin D, Amarillo Y*, et al.* Morphology and physiology of the polyaxonal amacrine cells in the rabbit retina. *J Comp Neurol*, 2001;440:109-125.
110. Xin D, Bloomfield SA. Comparison of the responses of AII amacrine cells in the dark- and light-adapted rabbit retina. *Vis Neurosci*, 1999;16:653-665.
111. Bloomfield SA, Xin D. Surround inhibition of mammalian AII amacrine cells is generated in the proximal retina. *J Physiol Lond*, 2000;15:771-783.
112. Sakai HM, Naka K. Response dynamics and receptive-field organization of catfish amacrine cells. *J Neurophysiol*, 1992;67(2):430-442.
113. Marc RE, Liu W. Fundamental GABAergic amacrine cell circuitries in the retina: nested feedback, concatenated inhibition, and axosomatic synapses. *J Comp Neurol*, 2000;425(4):560-82.
114. Petit-Jacques J, Bloomfield SA. Synaptic regulation of the light-dependent oscillatory currents in starburst amacrine cells of the mouse retina. *J Neurophysiol,* 2008:01399.2007.
115. Smith RG. Contributions of horizontal cells. In: Masland RH, Albright T, Eds. *The Senses: A comprehensive reference. Vision*. Amsterdam: Elsevier, 2008;341-349.
116. Famiglietti EV. Polyaxonal amacrine cells of rabbit retina: size and distribution of PA1 cells. *J Comp Neurol*, 1991;316:406-421.
117. Famiglietti EV. Polyaxonal amacrine cells of rabbit retina: PA2, PA3, and PA4 cells. Light and electron microscopic studies with a functional interpretation. *J Comp Neurol*, 1992;316(4):422-46.
118. Pow DV. Transport is the primary determinant of glycine content in retinal neurons. *Journal of Neurochemistry*, 1998;70(6):2628-36.
119. Brecha NC. Peptide and peptide receptor expression in function in the vertebrate retina. In: Chalupa LM, Werner J, Eds. *The Visual Neurosciences*, Cambridge, MA: MIT Press, 2004: 334-354.
120. Dowling JE, Boycott BB. Organization of the primate retina: electron microscopy. *Proc R Soc Lond B Biol Sci*, 1966; 166:80-111.
121. Wässle, H. Decomposing a cone's output (Parallel processing). In: Masland RH, Albright T, Eds. *The Senses: A comprehensive reference. Vision*. Amsterdam. Elsevier. 2008.
122. Kolb H, Dekorver L. Midget ganglion cells of the parafovea of the human retina: a study by electron microscopy and serial section reconstructions. *J Comp Neurol*, 1991;303:617-636.
123. Allen RA. The retinal bipolar cells and their synapses in the inner plexiform layer. In: Straatsma BR, Hall MO, Allen RA*, et al.* Eds. *The Retina: Morphology, Functional and Clinical Characteristics*. Los Angeles, CA: University of California Press, 1969;101–143
124. Slaughter MM. Inhibition in the retina. In: Chalupa LM, Werner J, Eds. *The Visual*

Neurosciences. Cambridge, MA: MIT Press, 2004;355-368.
125. Tachibana M, Kaneko A. γ-aminobutyric acid exerts a local inhibitory action on the axon terminal of bipolar cells: evidence for negative feedback from amacrine cells. *ProcNatl Acad Sci USA,* 1987;84(10):3501-3505.
126. Fletcher EL, Koulen P, Wässle H. GABAA and GABAC receptors on mammalian rod bipolar cells. *J Comp Neurol*, 1998;396(3):351-365.
127. Fiegenspan A, Bormann J. Differential contributions of GABAA and GABAC receptors on rat retinal bipolar cells. *Proc Natl Acad Sci USA*, 1994;91:10893-10897.
128. Zhang J, Jung CS, Slaughter MM. Serial inhibitory synapses in retina. *Vis Neurosci*, 1997;14(3):553-563.
129. Wässle H, Koulen P, Brandstatter JH*, et al.* Glycine and GABA receptors in the mammalian retina. *Vision Research*, 1998;38:1411-1430.
130. Strettoi E. Mammalian rod pathways. In: Masland RH, Albright T, Eds. *The Senses: A comprehensive reference. Vision*. Amsterdam: Elsevier, 2008;303-311.
131. Bloomfield , Dacheux RF. Rod vision: pathways and processing in the mammalian retina. *Prog Retinal & Eye Res*, 2001;20:351-84.
132. Kolb H, Famiglietti EV, Jr.. Rod and Cone Pathways in the Retina of the Cat. *Investigative Ophthalmology*, 1974; 15:935-946.
133. Kolb H, Famiglietti EV. Rod and Cone Pathways in the Inner Plexiform Layer of Cat Retina. *Science*, 1975; 186:47-49.
134. Rieke F. Seeing in the dark: Retinal processing and absolute visual threshold. In: Masland RH, Albright T, Eds. *The Senses: A comprehensive reference. Vision*. Amsterdam: Elsevier, 2008;393-412.
135. Li W, Keung JW, Massey SC. Direct synaptic connections between rods and OFF cone bipolar cells in the rabbit retina. *J Comp Neurol*, 2004;474:1-12.
136. Tsukamoto Y, Morigiwa K, Ueda M*, et al.* Microcircuits for night vision in mouse retina. *J Neurosci*, 2001;21:8616-8623.
137. Soucy E, Wang Y, Nirenberg S*, et al.* A novel signaling pathway from rod photoreceptors to ganglion cells in mammalian retina. *Neuron*, 1998;21:481-493.
138. Protti DA, Flores-Herr N, Li W*, et al.* Light signaling in scotopic conditions in the rabbit, mouse and rat retina: A physiological and anatomical study. *J Neurophysiol,* 2005;93:3479-3488.
139. Nelson R, Kolb H. A17: a broad-field amacrine cell in the rod system of the cat retina. *J Neurophysiol*, 1985;54:592-614.
140. Vaney DI. Morphological identification of serotonin-accumulating neurons in the living retina. *Science.*, 1986;233:444-446.
141. Vaney DI. The mosaic of amacrine cells in the mammalian retina. *Progress in retinal research*, New York. Pergamon. 1990, 49–100.
142. Zhang J, Li W, Trexler EB*, et al.* Confocal analysis of reciprocal feedback at rod bipolar terminals in the rabbit retina. *J Neurosci*, 2002;22:10871-10882.
143. Zhou C, Dacheux RF. All amacrine cells in the rabbit retina possess AMPA-, NMDA-, GABA-, and glycine-activated currents. *Vis Neurosci*, 2004;21:181-188.
144. Deans MR, Volgyi B, Goodenough DA*, et al.* Connexin36 Is Essential for Transmission of Rod-Mediated Visual Signals in the Mammalian Retina. *Neuron*, 2002;36:703-712.
145. Berson DM. Retinal ganglion cell types and their central projections. In: Masland RH, Albright T, Eds. *The Senses: A comprehensive reference. Vision*. Amsterdam: Elsevier, 2008;491-519.
146. Marc RE, Jones BW. Molecular phenotyping of retinal ganglion cells. *J Neurosci*, 2002;22:413-427.
147. Rockhill RL, Daly FJ, MacNeil MA*, et al.* The diversity of ganglion cells in a mammalian retina. *J Neurosci*, 2002;22:3831–3843.
148. Hartline HK. The response of single optic nerve fibers of the vertebrate eye to illumination of the retina. *Am J Physiol*, 1938; 121:400-415.
149. Kuffler SW. Discharge patterns and functional organization of mammalian retina. *J Neurophysiol*, 1953; 16:37-68.
150. Nelson R, Famiglietti EV Jr., Kolb H. Intracellular staining reveals different levels of stratification for On-Center and Off-Center ganglion cells in cat retina. *J Neurophysiol*, 1978; 41:472-483.

151. Naka K. Functional organization of catfish retina. *J Neurophysiol*, 1977; 40:26-43.
152. Enroth-Cugell C, Robson JG. The contrast sensitivity of retinal ganglion cells of the cat. *J Physiol*, 1966; 187:517-552.
153. Stone J, Hoffman KP. Conduction velocity as a parameter in the organisation of the afferent relay in the cat's lateral geniculate nucleus. *Brain Res Rev*, 1971; 32:454-459.
154. Stone J, Fukuda Y. Properties of cat retinal ganglion cells: a comparison of W-cells with X- and Y-cells. *J Neurophysiol*, 1974; 37:722-748.
155. Boycott BB, Wässle H. The morphological types of ganglion cells of the domestic cat's retina. *J Physiol*, 1974; 240:397-419.
156. Cleland BG, Levick WR. Properties of rarely encountered types of ganglion cells in the cat's retina and on overall classification. *J Physiol*, 1974; 240:457-492.
157. Provencio I. Melanopsin cells. In: Masland RH, Albright T, Eds. *The Senses: A comprehensive reference. Vision*. Amsterdam: Elsevier, 2008;423-431.
158. Famiglietti EV Jr. Wide-field cone bipolar cells and the blue-ON pathway to color-coded ganglion cells in rabbit retina. *Vis Neurosci*, 2008;25:53-66.
159. Lee BB. Blue-ON Cells. In: Masland RH, Albright T, Eds. *The Senses: A comprehensive reference. Vision*. Amsterdam: Elsevier, 2008;433-438.
160. Chatterjee S, Callaway EM. Parallel colour-opponent pathways to primary visual cortex. *Nature*, 2003;426:668-671.
161. Dacey DM, Liao HW, Peterson BB*, et al.* Melanopsin-expressing ganglion cells in primate retina signal colour and irradiance and project to the LGN. *Nature*, 2005;433:749-754.
162. Hattar S, Liao HW, Takao M*, et al.* Melanopsin-Containing Retinal Ganglion Cells: Architecture, Projections, and Intrinsic Photosensitivity. *Science*, 2002;295:1065-1070.
163. Guler AD, Ecker JL, Lall GS*, et al.* Melanopsin cells are the principal conduits for rod-cone input to non-image-forming vision. *Nature*, 2008;453:102-105.
164. Schmidt TM, Taniguchi K, Kofuji P. Intrinsic and extrinsic light responses in melanopsin-expressing ganglion cells during mouse development. *J Neurophysiol*, 2008:00062.2008.
165. Walker MT, Brown RL, Cronin TW*, et al.* Photochemistry of retinal chromophore in mouse melanopsin. *Proc Natl Acad Sci*, 2008;105:8861-8865.
166. Carroll J, Jacobs GH. Mammalian photopigments. In: Masland RH, Albright T, Eds. *The Senses: A comprehensive reference. Vision*. Amsterdam: Elsevier, 2008;247-268.
167. Kaplan E. The P, M and K streams of the primate visual system: What do they do for vision? In: Masland RH, Albright T, Eds. *The Senses: A comprehensive reference. Vision*. Amsterdam: Elsevier, 2008;369-381.
168. Smallwood PM, Wang Y, Nathans J. Role of a locus control region in the mutually exclusive expression of human red and green cone pigment genes. *Proc Natl Acad Sci*, 2002;99:1008-1011.
169. Wang Y, Smallwood PM, Cowan M*, et al.* Mutually exclusive expression of human red and green visual pigment-reporter transgenes occurs at high frequency in murine cone photoreceptors. *Proc Natl Acad Sci*, 1999;96:5251-5256.
170. Dacey DM. Parallel pathways for spectral coding in primate retina. *Annu. Rev. Neurosci*, 2000;23:743–775.
171. Calkins DJ, Sterling P. Absence of spectrally specific lateral inputs to midget ganglion cells in primate retina. *Nature*, 1996;381:613-615.
172. Reid RC, Shapley RM. Spatial structure of cone inputs to receptive fields in primate lateral geniculate nucleus. *Nature*, 1992;356:716-718.
173. Reid RC, Shapley RM. Space and time maps of cone photoreceptor signals in macaque lateral geniculate nucleus. *J Neurosci*, 2002;22:6158-6175.
174. Sun H, Smithson HE, Zaidi Q*, et al.* Specificity of cone inputs to macaque retinal ganglion cells. *J Neurophysiol* 2006;95:837-849.
175. Ledbedev DS, Marshak DW. Amacrine cell contributions to red-green color opponency in central primate retina: a model study. *Vis Neurosci* 2007; 24:535-547.
176. Svaetichin G, MacNichol EF. Retinal mechanisms for chromatic and achromatic

vision. *Ann NY Acad Sci*, 1958; 74:385-404.
177. Wyatt HJ, Daw NW. Directionally sensitive ganglion cells in the rabbit retina: specificity for stimulus direction, size, and speed. *J Neurophysiol*, 1975; 38:613-626.
178. Barlow HB, Hill RM, Levick WR. Retinal ganglion cells responding selectively to direction and speed of image motion in the rabbit. *J Physiol*, 1964; 173:377-407.
179. Dacheux RF, Chimento MF, Amthor FR. Synaptic input to the on-off directionally selective ganglion cell in the rabbit retina. *J Comp Neurol*, 2003;456:267-278.
180. Famiglietti EV Jr. On and off pathways through amacrine cells in mammalian retina: the synaptic connections of "starburst" amacrine cells. *Vision Res*, 1983;23:1265-1279.
181. Dmitrieva NA, Lindstrom JM, Keyser KT. The relationship between GABA-containing cells and the cholinergic circuitry in the rabbit retina. *Vis Neurosci*, 2001;18:93-100.
182. Famiglietti EV Jr. Dendritic co-stratification of ON and ON-OFF directionally selective ganglion cells with starburst amacrine cells in rabbit retina. *J Comp Neurol*, 1992;324:322-335.
183. Famiglietti EV Jr. A structural basis for omnidirectional connections between starburst amacrine cells and directionally selective ganglion cells in rabbit retina, with associated bipolar cells. *Vis Neurosci*, 2002;19:145-162.
184. Grzywacz NM, Amthor FR, Merwine DK. Necessity of acetylcholine for retinal directionally selective responses to drifting gratings in rabbit. *J Physiol*, 1998;512:575-81.
185. Caldwell JH, Daw NW, Wyatt HJ. Effects of picrotoxin and strychnine on rabbit retinal ganglion cells: lateral interactions for cells with more complex receptive fields. *J Physiol*, 1978; 276:277-298.
186. Kittila CA, Massey SC. Pharmacology of directionally selective ganglion cells in the rabbit retina. *J Neurophysiol*, 1997;77:675-689.
187. Oyster CW, Barlow HB. Direction-selective units in rabbit retina: distribution of preferred directions. *Science*, 1967; 155:841-842.
188. Rodieck R., *The First Steps in Seeing*: Sinaur. 1998.
189. Werblin FS, Dowling JE. Organization of the retina of the mudpuppy Necturus maculosus: II. Intracellular recording. *J Neurophysiol*, 1969; 32:339-355.
190. Eliasof S, Barnes S, Werblin FS. The interaction of ionic currents mediating single spike activity in retinal amacrine cells of the tiger salamander. *J Neurosci*, 1987;7:3512.
191. Lukasiewicz P, Werblin FS. A slowly inactivating potassium current truncates spike activity in ganglion cells of the tiger salamander retina. *J Neurosci*, 1988;8:4470-4481.
192. Mittman S, Taylor WR, Copenhagen DR. Concomitant activation of two types of glutamate receptor mediates excitation of salamander retinal ganglion cells. *J Physiol*, 1990;428:275-297.
193. Jacoby R, Stafford D, Kouyama N, *et al*. Synaptic inputs to ON parasol ganglion cells in the primate retina. *J Neurosci*, 1996;16:8041.
194. Awatramani GB, Slaughter MM. Origin of transient and sustained responses in ganglion cells of the retina. *J Neurosci*, 2000;20:7087.
195. Kaczmarek LK, Levitan IB. *Neuromodulation. The Biochemical Control of Neuronal Excitability*. New York: Oxford University Press. 1987.
196. Pin J-P, Duvoisin R. The metabotropic glutamate receptors: structure and functions. *Neuropharmacology*, 1995;34.
197. Koulen P, Kuhn R, Wässle H, *et al*. Modulation of the intracellular calcium concentration in photoreceptor terminals by a presynaptic metabotropic glutamate receptor. *Proc Natl Acad Sci USA*, 1999;96:9909-9914.
198. Eldred WD, Blute TA. Imaging of nitric oxide in the retina. *Vision Res*, 2005;45:3469–3486.
199. Nguyen-Legros J. Morphology and distribution of catecholamine neurons in mammalian retina. *Progress in retinal research*, 19887:113–147.
200. Witkovsky P, Schütte M. The organization of dopaminergic neurons in vertebrate retinas. *Vis Neurosci*, 1991;7:113-124.

201. Dacey DM. The dopaminergic amacrine cell. *J Comp Neurol*, 1990;301: :461–489.
202. Zhang D-Q, Zhou T-R, McMahon DG. Functional heterogeneity of retinal dopaminergic neurons underlying their multiple roles in vision. *J Neurosci*, 2007;27:692-699.
203. Critz SD, Marc RE. Glutamate antagonists that block hyperpolarizing bipolar cells increase the release of dopamine from turtle retina. *Vis Neurosci*, 1992;9:271-278.
204. O'Connor P, Dorison SJ, Watling KJ*, et al.* Factors affecting release of 3H-dopamine from perfused carp retina. *J Neurosci*, 1986;6:1857-1865.
205. Boatright JH, Rubim NM, Iuvone PM. Regulation of endogenous dopamine release in amphibian retina by melatonin: the role of GABA. *Vis Neurosci*, 1994;11:1013-1018.
206. Marc RE, Jones BW, Pandit P*, et al.* Excitatory drive patterns of TH1 dopaminergic polyaxonal cells in rabbit retina. *Invest Ophthalmol Vis Sci*, 2008;49:2432.
207. Hokoc JN, Mariani AP. Tyrosine hydroxylase immunoreactivity in the rhesus monkey retina reveals synapses from bipolar cells to dopaminergic amacrine cells. *J Neurosci*, 1987;7:2785-2793.
208. Witkovsky P, Nicholson, C, Rice ME, *et al.* Extracellular dopamine concentration in the retina of the clawed frog, Xenopus laevis. *Proc Natl Acad Sci USA*, 1993;90:5667-5671.
209. Bjelke B, Goldstein M, Tinner B*, et al.* Dopaminergic transmission in the rat retina: evidence for volume transmission. *J Chem Neuroanat*, 1996;12:37.
210. Iuvone P. Regulation of retinal dopamine biosynthesis and tyrosine hydroxylase activity by light. *Fed Proc*, 1984;43:2709.
211. Haycock JW, Haycock DA. Tyrosine hydroxylase in rat dopaminergic nerve terminals: multiple phosphorylation in vivo and in synaptosomes. *J Biol Chem*, 1991;266:5650.
212. Witkovsky P, Gabriel R, Haycock JW*, et al.* Influence of light and neural circuitry on tyrosine hydroxylase phosphorylation in the rat retina. *J Chem Neuroanat*, 2000;19:105.
213. Feigenspan A, Gustincich S, Bean BP*, et al.* Spontaneous activity of solitary dopaminergic cells of the retina. *J Neurosci*, 1998;18:6776–6789.
214. Xiao J, Cai Y, Yen J*, et al.* Voltage-clamp analysis and computational model of dopaminergic neurons from mouse retina. *Vis Neurosci*, 2004;21:835–849.
215. Witkovsky P. Dopamine and retinal function. *Doc Ophthalmol*, 2004;108:17–39.
216. Vaquero CF, Pignatelli A, Partida GJ*, et al.* A dopamine- and protein kinase A-dependent mechanism for network adaptation in retinal ganglion cells. *J Neurosci*, 2001;21:8624-8635.
217. Hampson EC, Vaney DI, Weiler R. Dopaminergic modulation of gap junction permeability between amacrine cells in mammalian retina. *J Neurosci*, 1992;12:4911–4922.
218. Hampson EC, Weiler R, Vaney DI. pH-Gated dopaminergic modulation of horizontal cell gap junctions in mammalian retina. *Proc Roy Soc B*, 1994;255:67-72.
219. Hayashida Y, Ishida AT. Dopamine receptor activation can reduce voltage-gated Na+ current by modulating both entry into and recovery from inactivation. *J Neurophysiol*, 2004;92:3134-3141.
220. Gustincich S, Contini M, Gariboldi M*, et al.* Gene discovery in genetically labeled single dopaminergic neurons of the retina. *Proc Natl Acad Sci U S A*, 2004;101:5069-5074.
221. Guo-Xiang R, Dao-Qi Z, Tongrong Z*, et al.* Circadian organization of the mammalian retina. *Proc Natl Acad Sci*, 2006;103:9703-9708.
222. Dorenbos R, Contini M, Hirasawa H*, et al.* Expression of circadian clock genes in retinal dopaminergic cells. *Vis Neurosci*, 2007;24:573-580.
223. Cahill GM, Besharse JC. Resetting the circadian clock in cultured Xenopus eyecups: regulation of retinal melatonin rhythms by light and D2 dopamine receptors. *J Neurosci*, 1991;11:2959-2971.
224. Besharse JC, Dunis DA. Methoxyindoles and photoreceptor metabolism: activation of rod shedding. *Science*, 1983;219:1341-1343.
225. Vugler AA, Redgrave P, Semo Ma*, et al.* Dopamine neurones form a discrete plexus with melanopsin cells in normal and de-

generating retina. *Experimental Neurology*, 2007;205:26-35.
226. Sakamoto K, Liu C, Kasamatsu M*, et al.* Dopamine regulates melanopsin mRNA expression in intrinsically photosensitive retinal ganglion cells. *Eur J Neurosci*, 2005;22:3129-3136.
227. Zhang DQ, Wong KY, Berson DM*, et al.* Sustained dopaminergic amacrine cells: Evidence for inputs From melanopsin ganglion-cell photoreceptors. *Invest Ophthalmol Vis Sci*, 2008;49:1517.
228. Descarries L, Bérubé-Carrière N, Riada M*, et al.* Glutamate in dopamine neurons: Synaptic versus diffuse transmission. *Brain Res Rev*, 2007, epub ahead of print.
229. O'Brien JJ, Li W, Pan F*, et al.* Coupling between A-Type horizontal cells Is mediated by connexin 50 gap junctions in the rabbit retina. *J Neurosci*, 2006;26:11624-11636.
230. Shelley J, Dedek K, Schubert T*, et al.* Horizontal cell receptive fields are reduced in connexin57-deficient mice. *Eur J Neurosci*, 2006;23:3176-3186.
231. Lasater EM, Dowling JE. Dopamine decreases conductance of the electrical junctions between cultured horizontal cells. Proc Natl Acad Sci USA 82:3025, 1985. *Proc Natl Acad Sci USA*, 1985;82:3025-3029.
232. Piccolino M, Neyton J, Gerschenfeld HM. Decrease of gap junction permeability induced by dopamine and cyclic adenosine 3':5' monophosphate in horizontal cells of turtle retina. *J Neurosci*, 1984;4:2477-2488.
233. Kothmann WW, Li X, Burr GS*, et al.* Connexin 35/36 is phosphorylated at regulatory sites in the retina. *Vis Neurosci*, 2007;24:363-375.
234. Lu C, McMahon DG. Modulation of retinal gap junction channel gating by nitric oxide. *J Physiol Lond*, 1997;499:689.
235. Weiler R, He S, Vaney DI. Retinoic acid modulates gap junctional permeability between horizontal cells of the mammalian retina. *Eur J Neurosci*, 1999;11:3346-3350.
236. Krizaj D, Gabriel R, Owen WG*, et al.* Dopamine D2 receptor-mediated modulation of rod-cone coupling in the *Xenopus* retina. *J Comp Neurol*, 1998;398:529.
237. Pozdeyev N, Tosini G, Li L*, et al.* Dopamine modulates diurnal and circadian rhythms of protein phosphorylation in photoreceptor cells of mouse retina. *Eur J Neurosci*, 2008;27:2691-2700.
238. Newman EA. Inward-rectifying potassium channels in retinal glial (Müller) cells. *J Neurosci*, 1993;13:3333-3345.
239. Barbour B, Brew H, Attwell D. Electrogenic uptake of glutamate and asparte into glial cells isolated from the salamander (*Ambystoma*) retina. *J Physiol Lond*, 1991;436:169-193.
240. Marc RE, Lam DM. Uptake of aspartic and glutamic acid by photoreceptors in goldfish retina. *Proc Natl Acad Sci USA*, 1981;78:7185-7189.
241. Ishida AT, Fain GL. D-aspartate potentiates the effects of L-glutamate on horizontal cells in goldfish retina. *Proc Natl Acad Sci U S A*, 1981;78:5890-5894.
242. Pow DV, Robinson SR. Glutamate in some retinal neurons is derived solely from glia. *Neuroscience*, 1994;60:355-366.
243. Pow DV, Crook DK. Direct immunocytochemical evidence for the transfer of glutamine from glial cells to neurons: Use of specific antibodies directed against thed-stereoisomers of glutamate and glutamine. *Neuroscience*, 1996;70:295-302.
244. Sarthy VP, Marc RE, Pignataro L*, et al.* Contribution of a glial glutamate transporter to GABA synthesis in the retina. *NeuroReport*, 2004;15:1895-1898.
245. Puro DG, Uyan JP, Sucher NJ. Activation of NMDA receptor-channels in human retinal Muller glial cells inhibits inward-rectifying potassium currents. *Vis Neurosci*, 1996;13:319.
246. Pachter JA, Lam DM. Interactions between vasoactive intestinal peptide and dopamine in the rabbit retina: stimulation of a common adenylate cyclase. *J Neurochem*, 1986;46:257-264.
247. Puro DG. Growth factors and Muller cells. *Prog Ret Eye Res*, 1995;15:89-101.
248. Newman EA. High potassium conductance in astrocyte endfeet. *Science*, 1986;233:453-454.
249. Newman EA, Zahs KR. Modulation of neuronal activity by glial cells in the retina. *J Neurosci*, 1998;18:4022-4028.

250. Newman EA. Glial modulation of synaptic transmission in the retina. *Glia*, 2004;47:268-274.
251. Howell GR, Libby RT, Jakobs TC*, et al*. Axons of retinal ganglion cells are insulted in the optic nerve early in DBA/2J glaucoma. *J. Cell Biol.*, 2007;179:1523-1537.
252. Bosco A, Inman DM, Steele MR*, et al*. Reduced Retina Microglial Activation and Improved Optic Nerve Integrity with Minocycline Treatment in the DBA/2J Mouse Model of Glaucoma. *Invest Ophthalmol Vis Sci*, 2008;49:1437-1446.
253. Tosini G, Menaker M. The clock in the mouse retina: melatonin synthesis and photoreceptor degeneration. *Brain Research*, 1998;789:221-228.
254. Cahill GM, Grace M,S Besharse JC. Rhythmic regulation of retinal melatonin: metabolic pathways, neurochemical mechanisms, and the ocular circadian clock. *Cell Mol Neurobiol*, 1991;11:529-560.
255. Tian N, Copenhagen DR. Visual Stimulation Is Required for Refinement of ON and OFF Pathways in Postnatal Retina. *Neuron*, 2003;39:85-96.
256. Tian N, Copenhagen D. Plasticity of retinal circuitry. In: Masland RH, Albright T, Eds. *The Senses: A comprehensive reference. Vision*. Amsterdam: Elsevier, 2008;473-490.
257. Pinaud R, Tremere LA, Penner MR*, et al*. Plasticity-driven gene expression in the rat retina. *Molec Brain Res*, 2002;98:93-101.
258. Pinaud R, De Weerd P, Currie RW*, et al*. Ngfi-a immunoreactivity in the primate retina: implications for genetic regulation of plasticity. *Int J Neurosci*, 2003, pageneeded1275-1285.
259. Marc RE, Jones BW, Watt CB*, et al*. Neural remodeling in retinal degeneration. *Progress in Retinal and Eye Research*, 2003;22:607-655.
260. Marc RE, Jones BW, Watt CB*, et al*. Extreme retinal remodeling triggered by light damage: Implications for AMD. *Molecular Vision*, 2008;14:782-806.
261. Tian N. Visual experience and maturation of retinal synaptic pathways. *Vision Res*, 2004;44:3307–3316.
262. Fisher SK, Lewis GP, Linberg KA*, et al*. Cellular remodeling in mammalian retina: results from studies of experimental retinal detachment. *Progress in Retinal and Eye Research*, 2005;24:395-431.
263. Rattner A, Nathans J. The genomic response to retinal disease and injury: Evidence for endothelin signaling from photoreceptors to glia. *J Neurosci*, 2005;25:4540-4549.
264. Buckingham BP, Inman DM, Lambert W*, et al*. Progressive ganglion cell degeneration precedes neuronal loss in a mouse model of glaucoma. *J Neurosci*, 2008;28:2735-2744.